Prepared for submission to JHEP
DESY 12-122

Multi-Regge Limit of the n-Gluon Bubble Ansatz

J. Bartels,[a] **V. Schomerus**[b] **and M. Sprenger**[b]

[a] *II. Institute for Theoretical Physics, Hamburg University, Germany*
[b] *DESY Theory Group, Hamburg, Germany*

E-mail: joachim.bartels@desy.de, volker.schomerus@desy.de, martin.sprenger@desy.de

Abstract: We investigate n-gluon scattering amplitudes in the multi-Regge region of $\mathcal{N} = 4$ supersymmetric Yang-Mills theory at strong coupling. Through a careful analysis of the thermodynamic bubble ansatz (TBA) for surfaces in AdS_5 with n-g(lu)on boundary conditions we demonstrate that the multi-Regge limit probes the large volume regime of the TBA. In reaching the multi-Regge regime we encounter wall-crossing in the TBA for all $n > 6$. Our results imply that there exists an auxiliary system of algebraic Bethe ansatz equations which encode valuable information on the analytical structure of amplitudes at strong coupling.

Keywords: AdS/CFT correspondence, scattering amplitudes, Bethe ansatz

Contents

1 Introduction

The computation of gluon scattering amplitudes in gauge theories such as Quantum Chromodynamics (QCD) or its supersymmetric cousins is a daunting task. Over the last few years much progress has been made in the context of $\mathcal{N} = 4$ supersymmetric Yang-Mills (SYM) theory, both at weak and strong coupling. These exciting developments exploit new hidden symmetries, such as dual conformal symmetry [1], and the celebrated duality with string theory on $AdS_5 \times S^5$

[2]. There is some hope to find expressions for the amplitudes that are valid for all values of the t'Hooft coupling, at least in the multi-color limit.

Such hopes were first nurtured by the intriguing BDS formula of Bern, Dixon and Smirnov [3]. It encapsulates the known infrared and collinear behavior of n-particle maximally helicity violating (MHV) amplitudes in the planar approximation. The authors of [3] conjectured the BDS formula to determine the amplitudes at each loop order $L \geq 2$, possibly up to some additive finite function $R^{(n)}$ of the kinematic variables, the so-called remainder function. Initially, $R^{(n)}$ was suspected to vanish, i.e. the BDS formula was believed to be exact.

Both gauge and string theory arguments subsequently confirmed this suspicion for $n = 4, 5$. In the weakly coupled theory, perturbative computations uncovered the before mentioned dual conformal symmetry of scattering amplitudes [1]. It implies that the remainder functions $R^{(n)}$ can only depend on conformal cross ratios, i.e. on conformally invariant combinations of the usual kinematic variables. Since there are no such cross ratios for $n = 4, 5$, the corresponding remainder functions have to be trivial. In other words, dual conformal invariance predicts that the BDS formula is exact for $n = 4, 5$ to all loop orders. This prediction was confirmed by a string theory computation of the leading term at strong coupling [4]. We shall say a bit more about the string theoretic analysis below.

On the other hand, the remainder function $R^{(n)}$ is now known to be non-zero for $n > 5$ and beyond one loop [5, 6]. Several authors have described tests of the BDS formula that exclude a vanishing remainder function. One of the most direct ways to see that $R^{(n)} \neq 0$ is based on a study of the SYM scattering amplitudes in the leading logarithmic approximation, see [7, 8]. The high energy (Regge) limit probes the remainder function near special points in the space of kinematic variables. While the Regge limit of the function $R^{(6)}$ vanishes at some of these points, for example when the limit is taken with all energies negative, the authors of [7, 8] were able to identify one region in which the Regge limit of $R^{(6)}$ is non-zero. Hence, $R^{(6)}$ must be a non-vanishing function of the kinematic variables. The analysis shows how computations in the Regge limit can provide strong and highly efficient constraints on the remainder function and its analytical structure.

In the meantime, the analytic expression [9] for the exact two-loop calculation of the six-point function [10, 11] was used to perform the relevant analytic continuation into the region with non-vanishing Regge limit [12]. The results are in full agreement with [8]. This settles the remainder function in the two-loop approximation, and it supports the all-order leading log generalization in [7, 8]. More recently, progress has been made with the extension of the calculation of $R_6^{(n)}$ to $n > 2$: in [13] the symbol of $R_6^{(3)}$ has been determined (up to two parameters), and in [14] this result has been confirmed, fixing also the two previously unknown constants. In [15] the authors quote results for the symbols of $R_6^{(n)}$ for four loops (again up to a number of unknown constants) [16]. The form of the scattering amplitudes in the Regge limit which, at weak coupling, was derived in the leading logarithmic approximation is quite general, and is expected to be valid also outside the weak coupling limit. As a function of the energy variables the amplitude contains Regge cut terms with power like dependence on s-like kinematic invariants (see below). The exponents depend on the kinematical region and are determined by the lowest eigenvalue of the BFKL color-octet Hamiltonian for an n-gluon system. These eigenvalues have recently been calculated in NLO accuracy in [17], and in [15] in next-to-next-to-leading order

(NNLO). The power-like energy dependence of the scattering amplitudes is multiplied by Regge impact factors which are now known also in NLO [18] and even in N^{3}LO accuracy [15]. A first generalization of the leading logarithmic analysis to the 7-point amplitude has been started in [19].

The BFKL color-octet Hamiltonian possesses the very interesting property that it coincides with the Hamiltonian of an integrable open spin chain [20] in leading order. Hence, the weakly coupled theory provides direct evidence for integrability in the high energy behaviour of planar scattering amplitudes.

Having reviewed all these results from gauge theory it is natural to ask what string theory has to say about the high energy limit of the remainder function $R^{(n)}$. In order to understand how the issue can be addressed, we need to briefly sketch the development that was initiated by the work [4] of Alday and Maldacena. The main insight of this paper was the identification of the leading contribution to an n-gluon amplitude at strong coupling with the area A_n of some 2-dimensional surface S_n inside AdS_5. According to the prescription of [4], S_n ends on a piecewise light-like polygon on the boundary of AdS_5. The light-like segments of this polygon are given by the momenta p_j of the external gluons. For $n = 4$ it is possible to find the surface explicitly and the resulting amplitude matches the prediction of the BDS formula. Constructing S_n for $n > 5$, however, turned out to be a rather difficult problem, at least for finite n and generic choice of the external momenta. The issue was resolved through a series of papers [21–23] in which the area of S_n is related to the free energy of some auxiliary quantum integrable system. More precisely, it was argued that A_n may be computed from a family of functions $\mathrm{Y}_{a,s}$ with $s = 1, 2, 3$ and $a = 1, \ldots, n-5$. The latter can be determined by solving a set of coupled non-linear integral equations. Very similar mathematical structures are familiar from the study of *ground states* in 1-dimensional quantum integrable systems on a circle of finite radius R. Moreover, the functional A_n resembles expressions for the free energy of such systems. So, in the sense we described, Alday et al. designed a 1-dimensional quantum integrable system such that its free energy computes the value of the remainder function $R^{(n)}$ at strong coupling. In the 1-dimensional theory one can tune $n-5$ complex mass parameters and the same number of real chemical potentials. The dependence of the free energy on these parameters captures the dependence of $R^{(n)}$ on the relevant kinematic variables.

Within the 1-dimensional quantum system it is natural to consider a limit in which the masses are sent to infinity or, equivalently, the volume R of the 1-dimensional space becomes large. In such a limit, all computations simplify once finite size corrections can be neglected. This applies in particular to the free energy of the ground state. The main goal of our work is to show that such a large volume limit of the 1-dimensional system possesses a nice re-interpretation in terms of the 4-dimensional gauge theory: It corresponds to the multi-Regge limit. Put differently, the map between 4-dimensional kinematic variables and parameters of the 1-dimensional system sends the multi-Regge regime to a point at which all the mass parameters become large. A more precise formulation of the limit in the 4-dimensional gauge theory will be given in section 2. The identification (5.2) of the corresponding regime in the auxiliary quantum system is one of the main results of this work. It is derived in sections 4,5 and generalizes previous observations [24] for the case of six gluons to an arbitrary number of external particles.

If we were only interested in the ground state energy of the system, the large mass limit would

be of limited interest. But it turns out that some excited states of the 1-dimensional quantum system also play an important role. In order to see them enter let us recall that the Regge limit of scattering amplitudes can be taken in different regions of the kinematic variables, such as the Euclidean region, the physical region where all energies are positive or 'mixed' physical regions with positive and negative energies. The limiting value of the remainder function depends on the region. In fact, when we pass from one region into another by continuation in the kinematic variables, the amplitude picks up Regge cut contributions that may have a non-vanishing high energy limit. In this sense, values of the remainder functions in the multi-Regge limit of different kinematic regions probe the analytical structure of the amplitude. One may wonder what all this corresponds to within the 1-dimensional auxiliary system. Since the kinematic variables are mapped to system parameters (masses and chemical potentials), we must vary the latter in order to move from one region of the kinematic variables to another. In the 1-dimensional system such a variation of system parameters can lead to a pair-wise creation of excitations above the ground state [25, 26]. The energy of such excited states may be non-zero in the large volume limit. Since the energy in the 1-dimensional system is related to the remainder function, *excitations* of the auxiliary model correspond to Regge cut contributions in the gauge theory. One example of this phenomenon was worked out in [24] for the case of six external gluons.

Combining the insights from the previous two paragraphs we must address the challenge of computing excitation energies in the infinite volume limit. When finite volume corrections can be neglected, excitation energies are determined by a set of algebraic Bethe ansatz equations. These replace the more complicated non-linear integral equations that govern a 1-dimensional integrable system at finite volume. The data that enter the Bethe ansatz equations, namely the momenta and $2 \mapsto 2$ scattering phases, can be derived from the non-linear integral equations. We will explain the general construction in section 6. In the case of six external gluons the derivation of the relevant Bethe ansatz is particularly simple so that we can make things very explicit. Starting from $n = 7$, an interesting new feature appears. In going to the multi-Regge regime of the 1-dimensional quantum system experiences wall-crossing, i.e. the associated non-linear integral equations pick up additional terms which we will compute in section 6. One can perform the large volume limit of such modified integral equations, but that leads to modifications in the Bethe ansatz, as well. More explanations and explicit formulas are included in section 6 along with a sketch of how one may proceed to bring the Bethe ansatz equations for $n \geq 7$ into the standard form.

From the point of the auxiliary quantum integrable system, the multi-Regge limit is opposite to the high-temperature (small mass, R) limit of the Y-system that was considered by Alday et. al. [23] and then studied in more detail in [27–29]. In terms of the 4-dimensional kinematics, the high-temperature limit corresponds to the case where the gluon momenta p_i form a regular polygon that can be embedded in a subspace $\mathbb{R}^{1,1}$ of the full momentum space $\mathbb{R}^{1,3}$. Another limiting regime of the kinematic variables is probed by the operator product expansions (OPE) of polygonal Wilson loops, see [30–32]. The information encoded in such Wilson loop OPEs seems more closely related to the multi-Regge limit, though the precise link is a bit difficult to establish even at weak coupling [33].

2 Multi-Regge kinematics

In this section we discuss the relevant variables and kinematics necessary for the description of $2 \to n-2$ scattering in the multi-Regge limit. The multi-Regge limit is characterized by the behaviour of a particular set of Mandelstam invariants. The remainder function of scattering amplitudes in $\mathcal{N}=4$ SYM theory, on the other hand, depends only on very special cross ratios of Mandelstam variables which are invariant under dual conformal symmetry. Our task here is to describe the multi-Regge limit in terms of such cross ratios.

2.1 Kinematic variables

We are interested in the scattering of two incoming particles with momenta $-p_1$, $-p_2$ resulting in a $(n-2)$-particle final state with outgoing momenta $p_3, ..., p_n$ as shown in figure 1. It will be convenient to label momenta p_i by arbitrary integers i such that $p_{i+n} = p_i$.

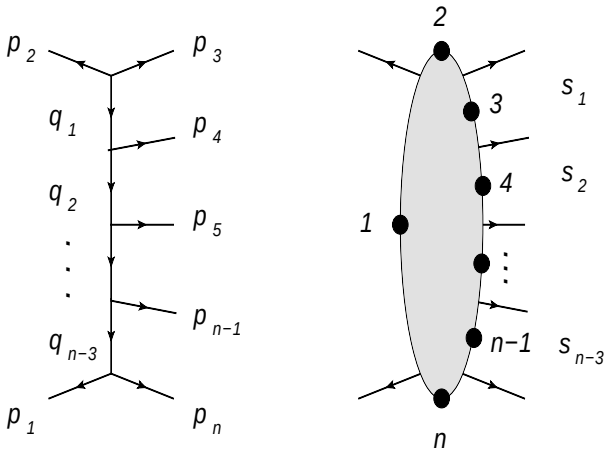

Figure 1. Kinematics of the scattering process $2 \to n-2$. On the right-hand side we show a graphical representation of the dual variables x_i.

In the context of $\mathcal{N}=4$ SYM theory it is advantageous to pass to a set of dual variables x_i such that

$$p_i = x_{i-1} - x_i. \tag{2.1}$$

The variables x_i inherit their periodicity $x_{i+n} = x_i$ from the periodicity of the p_i and momentum conservation. Let us also introduce the notation $x_{ij} = x_i - x_j$. The x_{ij} provide a large set of Lorentz invariants $x_{ij}^2 = x_{ji}^2$.[1] When expressed in terms of the momenta, these read

$$x_{ij}^2 = (p_{i+1} + \cdots + p_j)^2 . \tag{2.2}$$

[1] Throughout this paper we use the metric $(1, -1, -1, -1)$.

Obviously, only $3n-10$ Lorentz invariants are independent. Throughout this text we shall describe scattering processes through the $3n-10$ independent variables

$$t_r = x^2_{1,r+2} \ , \tag{2.3}$$

$$s_r = x^2_{r+1,r+3} \ , \tag{2.4}$$

$$\eta_p = \frac{x^2_{p-2,p}x^2_{p-1,p+1}}{x^2_{p-2,p+1}} \ , \tag{2.5}$$

where $r = 1, ..., n-3$ extends over all t-channels and $p = 4, ..., n-1$ labels the produced particles. In discussions of the multi-Regge limit it is actually quite common to use the cosines $z_r = \cos\theta_r$ of the scattering angle θ_r defined in the CM-system of the momentum q_r instead of s_r and to replace our variables η_p by the so-called Toller angles $\omega_{p\,p+1}$. With these choices, the multi-Regge limit is obtained by sending $z_r \to \infty$ with t_r and $\omega_{p\,p+1}$ held fixed. The variables we defined in eqs. (2.4) and (2.5) are more convenient (for a pedagogical discussion see [34]). In the variables (2.3)-(2.5) the multi-Regge limit is taken by sending s_r to infinity while keeping both t_r and η_p fixed.

As we recalled in the introduction, the missing remainder functions for gluon scattering in $\mathcal{N}=4$ SYM theory possess dual conformal symmetry. In other words, they only depend on conformally invariant combinations of Mandelstam variables. For an n-gluon scattering amplitude there are only $3n-15$ independent conformal invariants. We choose to work with the following set of cross ratios:

$$u_{1\sigma} = \frac{x^2_{\sigma+1,\sigma+5}x^2_{\sigma+2,\sigma+4}}{x^2_{\sigma+2,\sigma+5}x^2_{\sigma+1,\sigma+4}}, \tag{2.6}$$

$$u_{2\sigma} = \frac{x^2_{\sigma+3,n}x^2_{1,\sigma+2}}{x^2_{\sigma+2,n}x^2_{1,\sigma+3}}, \tag{2.7}$$

$$u_{3\sigma} = \frac{x^2_{2,\sigma+3}x^2_{1,\sigma+4}}{x^2_{2,\sigma+4}x^2_{1,\sigma+3}}, \tag{2.8}$$

where $\sigma = 1, ..., n-5$. For the $2 \to 5$ scattering process, a convenient graphical representation of the cross ratios is displayed in figure 2. Our main task now is to analyze the behavior of these $3n-15$ cross ratios in the multi-Regge limit.

2.2 Scattering in the center-of-mass system

To study the behaviour of the cross ratios in the multi-Regge limit we need some preliminary results which we will obtain by specializing to the CM-frame, writing the results in Lorentz invariant form. In our analysis throughout this subsection we shall study the behaviour of the set of subenergies

$$s_{i\cdots j} = (p_i + \cdots + p_j)^2 \ . \tag{2.9}$$

Note that these subenergies are the same as the Lorentz invariant variables $x^2_{ij} = s_{i+1\cdots j}$ we introduced in the previous subsection. The only reason we change notation here is to give the equations in this section a more familiar form. Subenergies s_{ii+1} for two adjacent particles of

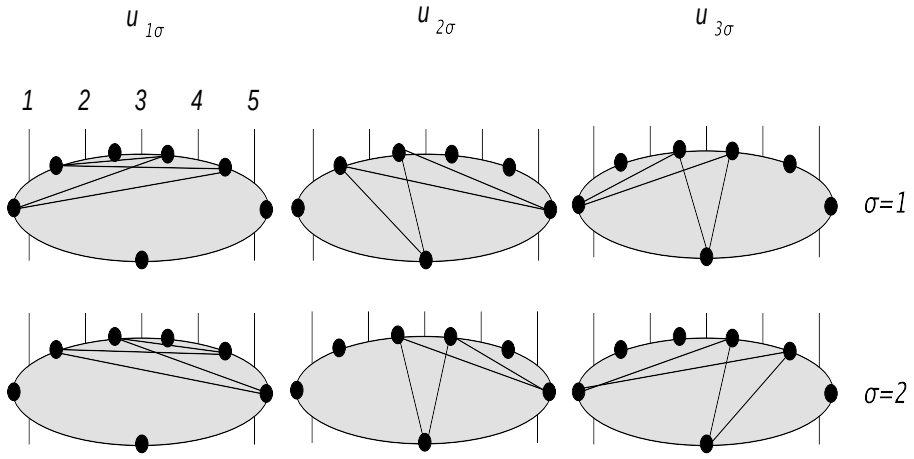

Figure 2. Graphical representation for the cross ratios of the 7-point amplitude.

momenta p_i and p_{i+1} are related to our variables s_r through $s_r = s_{r+2\,r+3}$. Furthermore, the total energy $s = (p_1 + p_2)^2$ of the process is given by $s = s_{3\cdots n}$.
In studying the Regge behaviour of the subenergies, it is useful to introduce the Sudakov parametrization

$$q_r = \delta_r \hat{p}_1 + \gamma_r \hat{p}_2 + q_{r\perp}, \tag{2.10}$$

for $r = 1, \ldots, n-3$. Here, $\hat{p}_1$ and $\hat{p}_2$ are light-like reference vectors from which we define our incoming momenta as $p_1 = -\hat{p}_1$, $p_2 = -\hat{p}_2$. They obey $2\hat{p}_1\hat{p}_2 = 2p_1p_2 = s$, and the transverse part, $q_{r\perp}$, is orthogonal to both $\hat{p}_1$ and $\hat{p}_2$, i.e. $\hat{p}_1 q_{r\perp} = \hat{p}_2 q_{r\perp} = 0$. A convenient frame is the CM-system of the incoming particles 1 and 2, with momenta $\hat{p}_1$ and $\hat{p}_2$ along the z-direction. We can determine the Sudakov parameters γ_r and δ_r by considering the following subenergies,

$$s_{3\cdots r+2} = (p_3 + \cdots + p_{r+2})^2 = (-p_2 - q_1 + q_1 - q_2 + \cdots + q_{r-1} - q_r)^2 = (p_2 + q_r)^2$$

$$s_{r+3\cdots n} = (p_{r+3} + \cdots + p_n)^2 = (q_r - q_{r+1} + q_{r+1} - \cdots + q_{n-3} - p_1)^2 = (p_1 - q_r)^2 \ .$$

Using that $q_i^2 = t_i$ we find

$$s_{3\cdots r+2} = 2q_r p_2 + t_r = -\delta_r s + t_r \quad \Rightarrow \quad \delta_r = \frac{t_r - s_{3\cdots r+2}}{s}, \tag{2.11}$$

as well as

$$s_{r+3\cdots n} = t_r - 2q_r p_1 \quad \Rightarrow \quad \gamma_r = \frac{s_{r+3\cdots n} - t_r}{s}. \tag{2.12}$$

Up to now all the identities have been exact. Now we would like to continue considering the multi-Regge limit which, as defined in the previous subsection, amounts to sending all pairwise energies $s_1, \ldots, s_{n-3}$ to infinity, while keeping both t- and η-variables fixed. In this paper we will restrict ourselves to the physical kinematic region where all energies are positive and all t_r negative (in a future study we we will consider also analytic continuations into other 'mixed' physical regions where some energies are negative). For the subenergies introduced in eq. (2.9) the multi-Regge limit implies

$$s \gg s_{3\cdots n-1}, s_{4\cdots n} \gg s_{3\cdots n-2}, \ldots, s_{5\cdots n} \gg \cdots \gg s_1, \ldots, s_{n-3} \gg -t_1, \ldots, -t_{n-3}. \tag{2.13}$$

From this well-known hierarchy of energy variables along with eqs. (2.11) and (2.12) one deduces the strong ordering of the Sudakov parameters γ_i and δ_i

$$1 \gg \gamma_1 \gg \gamma_2 \gg \cdots \gg \gamma_{n-3} \tag{2.14}$$

and

$$1 \gg -\delta_{n-3} \gg -\delta_{n-4} \gg \cdots \gg -\delta_1. \tag{2.15}$$

As a simple consequence of eqs. (2.11) and (2.12) we note that in the multi-Regge limit

$$t_r = q_r^2 = s\gamma_r\delta_r + q_{r\perp}^2 \cong q_{r\perp}^2, \tag{2.16}$$

where we could drop the term $s\gamma_r\delta_r \cong -s^{-1}s_{3\cdots r+2}s_{r+3\cdots n}$ because of the strong ordering (2.13) of subenergies in the multi-Regge limit. In conclusion, the finiteness of the t_r in the multi-Regge limit implies that the transverse components of the q_r stay finite. Since $p_{r+3} = q_r - q_{r+1}$ this is also true for the transverse components of the momenta p_{r+3} for $r = 1, \ldots, n-4$. We can compute this finite quantity from the mass-shell conditions of the produced particles with momenta $p_4, \ldots, p_{n-1}$:

$$\begin{aligned} 0 = p_p^2 = (q_{p-3} - q_{p-2})^2 \cong -s\gamma_{p-3}\delta_{p-2} + p_{p\perp}^2 = \frac{s_{3\cdots p}s_{p\cdots n}}{s} + p_{p\perp}^2 \\ \Rightarrow \frac{s_{3\cdots p}s_{p\cdots n}}{s} \cong -p_{p\perp}^2 = \vec{p}_p^{\,2}. \end{aligned} \tag{2.17}$$

We are now prepared to look at the subenergies in the multi-Regge limit. Let us begin with the subenergies formed by two adjacent particles. We have expressions of the form

$$\begin{aligned} s_r = (q_{r-1} - q_{r+1})^2 &\cong -s\gamma_{r-1}\delta_{r+1} + (p_{r+2} + p_{r+3})_\perp^2 \\ &\cong \frac{s_{3\cdots r+3}s_{r+2\cdots n}}{s} + (p_{r+2} + p_{r+3})_\perp^2 \end{aligned} \tag{2.18}$$

where r runs over $r = 2, ..., n-4$. Similarly, we can determine the leading terms in the multi-Regge limit of the subenergies for three adjacent particles,

$$\begin{aligned} s_{p-1\,p\,p+1} = (q_{p-4} - q_{p-1})^2 &\cong -s\gamma_{p-4}\delta_{p-1} + (p_{p-1} + p_p + p_{p+1})_\perp^2 \\ &\cong \frac{s_{3\cdots p+1}s_{p-1\cdots n}}{s} + (p_{p-1} + p_p + p_{p+1})_\perp^2 \end{aligned} \tag{2.19}$$

for $p = 5, ..., n-2$. As an application of these results we can now express the variables η_p in the multi-Regge limit through the momenta of produced particles. In order to do so, we express the basic definition (2.5) of the η variables through the subenergies (2.9). All three subenergies that appear in the expression can then be replaced by their leading behavior in the multi-Regge limit, i.e. the first term in eqs. (2.18) and (2.19), respectively. Comparing the resulting expression with the result (2.17) we arrive at

$$\eta_p = \frac{s_{p-3}s_{p-2}}{s_{p-1\,p\,p+1}} \cong -p_{p\perp}^2 = \vec{p}_p^{\,2}\ . \tag{2.20}$$

We can apply this result to derive a relation between our η variables and the (azimuthal) Toller angles between between adjacent vectors $\vec{q}_r$, $\vec{q}_{r+1}$. The angle between vectors $\vec{q}_r$ and $\vec{q}_{r+1}$ can be determined by computing

$$\vec{p}_{r+3}^{\,2} = (\vec{q}_r - \vec{q}_{r+1})^2 = |t_r| + |t_{r+1}| - 2\sqrt{|t_r||t_{r+1}|}\cos\theta_{r,r+1} \tag{2.21}$$

for $r = 1, \ldots, n-4$. According to eq. (2.20), the quantity $\vec{p}_{r+3}$ coincides with the variable η_{r+3} in the multi-Regge limit. Hence, we obtain

$$\cos\theta_{r,r+1} \cong \frac{|t_r| + |t_{r+1}| - \eta_{r+3}}{2\sqrt{|t_r||t_{r+1}|}}. \tag{2.22}$$

Below we shall need an explicit expression for the sine of the (azimuthal) Toller angle $\theta_{r,r+1}$ in the multi-Regge limit. It is given by

$$\sin\theta_{r,r+1} = \sqrt{1 - \cos^2\theta_{r,r+1}} \cong \frac{\lambda(|t_r|, |t_{r+1}|, \eta_{r+3})}{2\sqrt{|t_r||t_{r+1}|}}, \tag{2.23}$$

with

$$\lambda^2(|t_r|, |t_{r+1}|, \eta_{r+3}) = 2|t_r||t_{r+1}| + 2\eta_{r+3}|t_r| + 2\eta_{r+3}|t_{r+1}| - |t_r|^2 - |t_{r+1}|^2 - \eta_{r+3}^2. \tag{2.24}$$

From these angles between adjacent vectors $\vec{q}_r$ and $\vec{q}_{r+1}$ it is straightforward to compute the angles between arbitrary vectors $\vec{q}_r$ and $\vec{q}_{r'}$ due to the 2-dimensional kinematics in the multi-Regge limit.

So far, we have only looked at subenergies for up to three particles. But it is clear how to continue the analysis. Generalizing the derivations of our eqs. (2.18) or (2.19) we obtain

$$s_{r+2\ldots r'+3} \cong \frac{s_{r+2\cdots n} s_{3\cdots r'+3}}{s} + (p_{r+2} + \ldots p_{r'+3})_\perp^2 \,. \tag{2.25}$$

Comparison of the leading terms allow us to conclude that

$$s_{r+2\cdots r'+3} = (p_{r+2} + \cdots + p_{r'+3})^2 \cong \frac{s_r \cdots s_{r'}}{\eta_{r+3} \cdots \eta_{r'+2}} \,. \tag{2.26}$$

Note that for $r' = r+1$, i.e. when the subenergy on the left hand side involves three particles, the relation is exact and not restricted to the multi-Regge limit. For more than three particles contributing to the subenergy, on the other hand, the result (2.26) only describes the leading term and it takes more effort to determine the subleading term from eq. (2.25). In the next subsection we only need to determine the subleading contribution for very special combinations of subenergies. We postpone further discussion of such subleading terms until we have spelled out the relevant combinations.

2.3 Cross ratios in the multi-Regge limit

Let us now look at the behavior of the cross ratios defined by eqs. (2.6)-(2.8) in the multi-Regge limit. Combining eq. (2.26) with eq. (2.2) we obtain the leading term in the multi-Regge limit of the basic Lorentz invariants $x_{1+r,3+r'}^2$:

$$x_{1+r,3+r'}^2 = s_{r+2\cdots r'+3} \cong \frac{s_r \cdots s_{r'}}{\eta_{r+3} \cdots \eta_{r'+2}} \,. \tag{2.27}$$

If we insert this asymptotic behaviour into our definitions (2.7) and (2.8) for the cross ratios $u_{2\sigma}$ and $u_{3\sigma}$ we conclude

$$u_{2\sigma} = \frac{t_\sigma}{t_{\sigma+1}} \frac{x^2_{\sigma+3,n}}{x^2_{\sigma+2,n}} \cong \frac{t_\sigma}{t_{\sigma+1}} \frac{\eta_{\sigma+4}}{s_{\sigma+1}}, \tag{2.28}$$

$$u_{3\sigma} = \frac{t_{\sigma+2}}{t_{\sigma+1}} \frac{x^2_{2,\sigma+3}}{x^2_{2,\sigma+4}} \cong \frac{t_{\sigma+2}}{t_{\sigma+1}} \frac{\eta_{\sigma+3}}{s_{\sigma+1}} \ . \tag{2.29}$$

When we send s_σ to infinity to reach the multi-Regge regime, both sets of cross ratios go to zero. Since the coefficients of $1/s_\sigma$ depend on the $t-$ and η variables only, the ratios

$$\frac{u_{2\sigma}}{u_{3\sigma}} \cong \frac{t_\sigma}{t_{\sigma+2}} \frac{\eta_{\sigma+4}}{\eta_{\sigma+3}} \tag{2.30}$$

approach a non-vanishing constant value in the multi-Regge limit. Functions of the cross ratios that remain finite in the multi-Regge limit can therefore depend on the ratios $u_{2\sigma}/u_{3\sigma}$.
Let us now look at the remaining set of cross ratios $u_{1\sigma}$. Once more, we can rewrite our definition (2.6) in terms of the energy variables (2.9) using eq. (2.2) to obtain

$$u_{1\sigma} = \frac{s_{\sigma+2\cdots\sigma+5} s_{\sigma+3\ \sigma+4}}{s_{\sigma+3\cdots\sigma+5} s_{\sigma+2\cdots\sigma+4}} \ . \tag{2.31}$$

If we now insert the limiting behavior (2.26) for all four subenergies we see that all variables $u_{1\sigma}$ behave as $u_{1\sigma} \cong 1 + \ldots$. In order to obtain the leading non-trivial term in the multi-Regge limit we must work a little harder.
To this end we write, in analogy with eqs. (2.18)-(2.19), expressions for the subenergies $s_{\sigma+3\ \sigma+4}$, $s_{\sigma+3\cdots\sigma+5}$, $s_{\sigma+2\cdots\sigma+4}$, and $s_{\sigma+2\cdots\sigma+5}$. Beginning with the relation for $s_{\sigma+3\ \sigma+4}$

$$1 = \frac{s_{3\cdots\sigma+4} s_{\sigma+3\cdots n}}{s s_{\sigma+3\ \sigma+4}} + \frac{(p_{\sigma+3} + p_{\sigma+4})^2_\perp}{s_{\sigma+3\ \sigma+4}}, \tag{2.32}$$

we write

$$1 = \frac{s_{3\cdots\sigma+4} s_{\sigma+2\cdots n}}{s s_{\sigma+2\cdots\sigma+4}} \cdot \frac{s_{3\cdots\sigma+5} s_{\sigma+3\cdots n}}{s s_{\sigma+3\cdots\sigma+5}} \cdot \frac{s s_{\sigma+2\cdots\sigma+5}}{s_{3\cdots\sigma+5} s_{\sigma+2\cdots n}} \cdot \frac{s_{\sigma+2\cdots\sigma+4} s_{\sigma+3\cdots\sigma+5}}{s_{\sigma+3\ \sigma+4} s_{\sigma+2\cdots\sigma+5}} + \frac{(p_{\sigma+3} + p_{\sigma+4})^2_\perp}{s_{\sigma+3\ \sigma+4}}. \tag{2.33}$$

On the right-hand side, the fourth fraction equals $u^{-1}_{1\sigma}$, and the first three fractions are equal to unity, arising from the equations for $s_{\sigma+2\cdots\sigma+4}$, $s_{\sigma+3\cdots\sigma+5}$, and $s_{\sigma+2\cdots\sigma+5}$, with corrections of the order $\mathcal{O}(1/s_{\sigma+2\cdots\sigma+4})$, $\mathcal{O}(1/s_{\sigma+3\cdots\sigma+5})$, $\mathcal{O}(1/s_{\sigma+2\cdots\sigma+5})$, respectively. Compared to the last term in eq. (2.33), these corrections can be neglected and we are left with

$$u_{1\sigma} \cong 1 + \frac{(p_{\sigma+3} + p_{\sigma+4})^2_\perp}{s_{\sigma+3\ \sigma+4}} \tag{2.34}$$

with further corrections being smaller than $\mathcal{O}(1/s_{\sigma+3\ \sigma+4})$. The numerator of the correction term in eq. (2.34) can be expressed in terms of Lorentz invariants. To do so, we use the results of section 2.2 by writing

$$(\vec{p}_{\sigma+3} + \vec{p}_{\sigma+4})^2 = (\vec{q}_\sigma - \vec{q}_{\sigma+2})^2 = |t_\sigma| + |t_{\sigma+2}| - 2\sqrt{|t_\sigma||t_{\sigma+2}|}\cos(\theta_{\sigma,\sigma+1} + \theta_{\sigma+1,\sigma+2}), \tag{2.35}$$

which finally gives $(\vec{p}_{\sigma+3}+\vec{p}_{\sigma+4})^2=\rho_\sigma$ with a set of functions of the t and η variables defined by

$$\rho_\sigma(t,\eta):=|t_\sigma|+|t_{\sigma+2}|-2\sqrt{|t_\sigma||t_{\sigma+2}|}\left(\frac{|t_\sigma|+|t_{\sigma+1}|-\eta_{\sigma+3}}{2\sqrt{|t_\sigma||t_{\sigma+1}|}}\frac{|t_{\sigma+1}|+|t_{\sigma+2}|-\eta_{\sigma+4}}{2\sqrt{|t_{\sigma+1}||t_{\sigma+2}|}}\right.$$
$$\left.-\frac{\lambda(|t_\sigma|,|t_{\sigma+1}|,\eta_{\sigma+3})}{2\sqrt{|t_\sigma||t_{\sigma+1}|}}\frac{\lambda(|t_{\sigma+1}|,|t_{\sigma+2}|,\eta_{\sigma+4})}{2\sqrt{|t_{\sigma+1}||t_{\sigma+2}|}}\right)\,. \tag{2.36}$$

We can now summarize the findings of our analysis on the multi-Regge limit of the cross ratios $u_{1\sigma}$ through

$$u_{1\sigma}-1=\rho_\sigma(t,\eta)/s_{\sigma+1} \tag{2.37}$$

where we also changed notations back using $s_{\sigma+1}=s_{\sigma+3\,\sigma+4}$, as mentioned before. As in the case of the cross ratios $u_{2\sigma}$ and $u_{3\sigma}$ the leading correction to $u_{1\sigma}-1$ vanishes in the multi-Regge limit. But the following ratios remain finite

$$\frac{u_{1\sigma}-1}{u_{2\sigma}}\cong\frac{\rho_\sigma(t,\eta)t_{\sigma+1}}{t_\sigma\eta_{\sigma+4}}, \tag{2.38}$$

$$\frac{u_{1\sigma}-1}{u_{3\sigma}}\cong\frac{\rho_\sigma(t,\eta)t_{\sigma+1}}{t_{\sigma+2}\eta_{\sigma+3}}. \tag{2.39}$$

This concludes our description of the kinematics in the multi-Regge limit.

3 The n-gluon thermodynamic bubble ansatz

The main goal of this section is to review the Y-system for the computation of n-gluon amplitudes at strong coupling [22, 30]. In the first subsection we explain how the most interesting contribution to the scattering amplitude can be computed by solving a system of non-linear integral equations (NLIE). Then we relate the parameters of the NLIE to the cross ratios that were introduced in eqs. (2.6)-(2.8).

3.1 Amplitudes and the Y-system

We are interested in the calculation of scattering amplitudes in $\mathcal{N}=4$ SYM at strong coupling. To leading order they are given by

$$\text{Amplitude}\sim e^{-\frac{\sqrt{\lambda}}{2\pi}A}, \tag{3.1}$$

where A is the area of a minimal surface in AdS_5 with piece-wise light-like boundary. A general prescription for the calculation of this area A is given in [23, 35]. It contains a number of different pieces, including a divergent BDS-like term and a number of finite contributions. All but one of these terms can be spelled out explicitly. The remaining one is also known, but it is characterized somewhat indirectly through the solution of a coupled system of non-linear integral equations. Because of the resemblance with the way one describes the free energy of a 2-dimensional quantum integrable system, this contribution to the area A has been dubbed

A_{free}. In our analysis of the multi-Regge limit we can restrict to the discussion of this free energy contribution since the remaining terms are straightforward to include.
For our study of scattering amplitudes in the multi-Regge regime we need some more background on A_{free}. It can be calculated from a set of functions $\mathrm{Y}_{a,s}$ with $a = 1, 2, 3$ and $s = 1, \ldots, n-5$, which are determined as solutions of the following set of integral equations:

$$\log \mathrm{Y}_{1,s} = -m_s \cosh\theta - C_s - \frac{1}{2} K_2 \star \beta_s - K_1 \star \alpha_s - \frac{1}{2} K_3 \star \gamma_s, \tag{3.2}$$

$$\log \mathrm{Y}_{2,s} = -m_s \sqrt{2} \cosh\theta - K_2 \star \alpha_s - K_1 \star \beta_s, \tag{3.3}$$

$$\log \mathrm{Y}_{3,s} = -m_s \cosh\theta + C_s - \frac{1}{2} K_2 \star \beta_s - K_1 \star \alpha_s + \frac{1}{2} K_3 \star \gamma_s, \tag{3.4}$$

where $K \star f$ denotes the convolution integral

$$\int_{-\infty}^{\infty} d\theta' K(\theta - \theta') f(\theta') \tag{3.5}$$

and α_s, β_s, γ_s are given by

$$\alpha_s = \log \frac{(1+\mathrm{Y}_{1,s})(1+\mathrm{Y}_{3,s})}{(1+\mathrm{Y}_{2,s-1})(1+\mathrm{Y}_{2,s+1})}, \tag{3.6}$$

$$\beta_s = \log \frac{(1+\mathrm{Y}_{2,s})^2}{(1+\mathrm{Y}_{1,s-1})(1+\mathrm{Y}_{1,s+1})(1+\mathrm{Y}_{3,s-1})(1+\mathrm{Y}_{3,s+1})}, \tag{3.7}$$

$$\gamma_s = \log \frac{(1+\mathrm{Y}_{1,s-1})(1+\mathrm{Y}_{3,s+1})}{(1+\mathrm{Y}_{1,s+1})(1+\mathrm{Y}_{3,s-1})}. \tag{3.8}$$

The kernel function K_a are known to take the form

$$K_1 = \frac{1}{2\pi} \frac{1}{\cosh\theta} \quad , \quad K_2 = \frac{\sqrt{2}}{\pi} \frac{\cosh\theta}{\cosh 2\theta} \quad , \quad K_3 = \frac{i}{\pi} \tanh 2\theta. \tag{3.9}$$

Furthermore, m_s and C_s are constants that we need to determine in the following. These equations can be used for $|\mathrm{Im}\,\theta| \leq \frac{\pi}{4}$. For larger values of θ, we can either pick up pole contributions from the kernels or use the recursion relation

$$\mathrm{Y}_{a,s}^{[r]} = \frac{\left(1+\mathrm{Y}_{a,s+1}^{[r\pm1]}\right)\left(1+\mathrm{Y}_{4-a,s-1}^{[r\pm1]}\right)}{\mathrm{Y}_{4-a,s}^{[r\pm2]}\left(1+\frac{1}{\mathrm{Y}_{a+1,s}^{[r\pm1]}}\right)\left(1+\frac{1}{\mathrm{Y}_{a-1,s}^{[r\pm1]}}\right)}, \tag{3.10}$$

where we introduced the symbol $\mathrm{Y}_{a,s}^{[r]}(\theta) = \mathrm{Y}_{a,s}(\theta + ir\pi/4)$ for Y-functions with arguments shifted by multiples of $i\pi/4$. For the moment let us consider the m_s as complex parameters while we take C_s to be real. Consequently, the total number of real parameters in the eqs. (3.2)-(3.4) is $3(n-5)$, matching the number of independent cross ratios for n-gluon scattering. The precise relation between the cross ratios and the parameters m_s, C_s will be addressed in the next subsection. Right now it suffices to keep in mind that the parameters $m_s = m_s(u_{a\sigma})$

and $C_s = C_s(u_{a\sigma})$ in the Y-system need to be adjusted as we vary the kinematic variables.
Let us add a few more comments on complex mass parameters m_s. The correct way to interpret the Y-system in the presence of complex masses is through the following substitutions in the original equations:

$$m_s \to |m_s|\,, \quad \mathrm{Y}_{a,s}(\theta) \to \mathrm{Y}_{a,s}(\theta + i\phi_s), \quad K^{a,a'}_{s,s'}(\theta - \theta') \to K^{a,a'}_{s,s'}(\theta - \theta' + i(\phi_s - \phi_{s'})). \tag{3.11}$$

Here we have split each complex m_s into the real parameters $|m_s|$ and the phase ϕ_s. For $|\phi_s - \phi_{s'}| = n \cdot \frac{\pi}{4}$ the kernels become singular, and we have to pick up the corresponding poles. Such large phases are going to play an important role later on.
Once the solution $Y_{a,s}$ of the Y system has been found, we can compute the quantity A_{free} through the simple prescription

$$A_{\text{free}} = \sum_s \int \frac{d\theta}{2\pi} |m_s| \cosh\theta \log\left[(1+\mathrm{Y}_{1,s})\,(1+\mathrm{Y}_{3,s})\,(1+\mathrm{Y}_{2,s})^{\sqrt{2}}\right](\theta + i\phi_s)\,. \tag{3.12}$$

Note that A_{free} depends on the kinematic variables $u_{a\sigma}$ of the scattering process through the parameters m_s, ϕ_s and C_s of the auxiliary quantum integrable system.

3.2 Y-system and cross ratios

In this section we relate the cross ratios to the value of the Y-functions at special values of the spectral parameter θ. To do so, we follow [23] and define

$$U_s^{[r]} := 1 + \frac{1}{Y_{2,s}^{[r]}} := 1 + \frac{1}{\mathrm{Y}_{2,s}}\bigg|_{\theta = i\pi r/4} = 1 + \frac{1}{\mathrm{Y}_{2,s}^{[r]}}\bigg|_{\theta=0} \tag{3.13}$$

for $s = 1, \ldots, n-5$ and r any integer. These quantities possess a rather simple relation with the cross ratios. When both indices of U are even, one has

$$U_{2k-2}^{[2p]} = \frac{x^2_{-k+p,k+p}\, x^2_{-k+p-1,k+p-1}}{x^2_{-k+p-1,k+p}\, x^2_{-k+p,k+p-1}}\,. \tag{3.14}$$

Here $2k-2$ is the number of cusps between the pairs $\{x_{-k+p-1}, x_{-k+p}\}$ and $\{x_{k+p-1}, x_{k+p}\}$, see [23] for details. For sites separated by an odd number $2k-1$ of cusps, the relevant relation reads

$$U_{2k-1}^{[2p+1]} = \frac{x^2_{-k+p,k+p+1}\, x^2_{-k+p-1,k+p}}{x^2_{-k+p-1,k+p+1}\, x^2_{-k+p,k+p}}\,. \tag{3.15}$$

We can now insert the general relations (3.14) and (3.15) into our definition of the special cross ratios eqs. (2.6)-(2.8) to obtain

$$\begin{aligned}
u_{1\sigma} &= \frac{x^2_{\sigma+1,\sigma+5}\, x^2_{\sigma+2,\sigma+4}}{x^2_{\sigma+2,\sigma+5}\, x^2_{\sigma+1,\sigma+4}} = \left(U_1^{[2\sigma+7]}\right)^{-1} = \frac{Y_{2,1}^{[2\sigma+7]}}{1 + Y_{2,1}^{[2\sigma+7]}} \\
u_{2\sigma} &= \frac{x^2_{\sigma+3,n}\, x^2_{1,\sigma+2}}{x^2_{\sigma+2,n}\, x^2_{1,\sigma+3}} = \left(U_\sigma^{[\sigma+4]}\right)^{-1} = \frac{Y_{2,\sigma}^{[\sigma+4]}}{1 + Y_{2,\sigma}^{[\sigma+4]}} \\
u_{3\sigma} &= \frac{x^2_{2,\sigma+3}\, x^2_{1,\sigma+4}}{x^2_{1,\sigma+3}\, x^2_{2,\sigma+4}} = \left(U_\sigma^{[\sigma+6]}\right)^{-1} = \frac{Y_{2,\sigma}^{[\sigma+6]}}{1 + Y_{2,\sigma}^{[\sigma+6]}}.
\end{aligned} \tag{3.16}$$

The Y-functions appearing in our theory depend on the $3n-15$ parameters m_s, C_s, ϕ_s in the non-linear integral equations. Hence, $\mathrm{Y}_{a,s}^{[r]}$ which are just shifted Y-function evaluated at the origin of the θ plane, are functions of these parameters. The equations (3.16) describe the transformation between the parameters in the non-linear integral equations and the cross ratios of the scattering process. We can invert them, at least numerically, to determine m_s, C_s and ϕ_s from the kinematic invariants of the n-gluon system.
The formulae derived above for the cross ratios give rise to large values in the upper index of the Y-functions. As we shall see later, this is a bit of a nuisance for practical computations. It is therefore useful to observe that there exist two symmetries which may be used to reduce the value of the upper index. These symmetries have their origin in the $\mathbb{Z}_4$-symmetry of the underlying Hitchin system. The first of these symmetries reads

$$U_s^{[l]} = U_s^{[l\pm 2n]} \ . \tag{3.17}$$

Note that such a symmetry must necessarily hold in order for the identification (3.14) and (3.15) with cross ratios to be consistent with the symmetry $x_{i+n} = x_i$ of the x-variables. A second useful symmetry of the quantities $U_s^{[l]}$ is given by

$$U_s^{[l]} = U_{n-4-s}^{[l\pm n]} \ . \tag{3.18}$$

In this case, we must accompany the shift in the upper by a reflection in the lower index. Once again, the corresponding symmetry of cross ratios is easy to verify. With these symmetries, it is always possible to reduce the absolute value of the upper index of the Y-functions to $\lfloor \frac{n}{2} \rfloor$ or lower. In order to achieve further reduction, one can employ the recursion relations (3.10).

4 Multi-Regge limit of the TBA for $n \leq 7$ gluons

The multi-Regge limit was defined in section 2 through the dynamical invariants of the scattering process as a limit in which the s-variables are sent to infinity while t- and η-variables are held fixed. We have also analyzed how the special cross ratios (2.6)-(2.8) behave in the limit. In section 3 we then went on to discuss the relation (3.16) between cross ratios and the parameters of the non-linear integral equations. Our next task is to understand which limit of the parameters m_s, ϕ_s and C_s has to be taken in order for the cross ratios to show multi-Regge behavior. The case with $n = 6$ has been treated before [24] and is relatively simple to analyze. We will review some formulas in the next subsection before turning to $n > 6$ gluons. Beyond $n = 6$ there are some important new features in taking the multi-Regge limit. We will explain these first for the example of $n = 7$ before we delve into a general analysis in the subsequent section.

4.1 Review of the hexagon $n = 6$

In order to understand the basic steps of our analysis we would like to review briefly how things work in the case of 6 gluons [24]. For six points, there are three independent cross ratios:

$$u_1 = \frac{x_{35}^2 x_{26}^2}{x_{36}^2 x_{25}^2} = \frac{Y_2^{[-3]}}{1+Y_2^{[-3]}}, \qquad u_2 = \frac{x_{13}^2 x_{46}^2}{x_{14}^2 x_{36}^2} = \frac{Y_2^{[-1]}}{1+Y_2^{[-1]}}, \qquad u_3 = \frac{x_{15}^2 x_{24}^2}{x_{14}^2 x_{25}^2} = \frac{Y_2^{[1]}}{1+Y_2^{[1]}}.$$

We have omitted all the second indices for both u and Y because $\sigma = 1$ is the only value it can take when $n - 5 = 1$. From the kinematic analysis in section 2 we know that $u_1 \to 1$ in the multi-Regge limit, while u_2 and u_3 tend to zero. Comparing the expressions for the Y-functions with this limit, the authors of [24] show that

$$m \to \infty, \quad \phi \to 0, \quad C = \text{const.} \tag{4.1}$$

is the appropriate limit one has to perform in the non-linear integral equations in order for the cross ratios to assume their limiting values in the Regge regime. When the limit (4.1) is taken, the integrals in the NLIE (3.2)-(3.4) may be neglected. Consequently, we obtain a set of explicit expressions for the form of the Y-functions in the limiting regime:

$$\mathrm{Y}_1(\theta) \cong e^{-m\cosh(\theta - i\phi) - C}\ , \quad \mathrm{Y}_2(\theta) \cong e^{-m\sqrt{2}\cosh(\theta - i\phi)}\ , \quad \mathrm{Y}_3(\theta) \cong e^{-m\cosh(\theta - i\phi) + C}\ .$$

Recall that these expressions should only be used for $|\mathrm{Im}\theta| < \pi/4$. Outside this fundamental strip one needs to apply the recursion relations (3.10) to bring the arguments back into the strip. Before we insert these expressions into the formulas (3.16) let us replace m and ϕ by the new variables

$$\epsilon = e^{-m\cos\phi}, \quad w = e^{m\sin\phi}, \tag{4.2}$$

which behave as $\epsilon \to 0$ and $w \to$ const. in the limit (4.1). In terms of these new parameters, the cross ratios (3.16) can be expanded as

$$u_1 = 1 - \left(w + \frac{1}{w} + 2\cosh C\right)\epsilon + \mathcal{O}(\epsilon^2), \qquad u_2 = w\epsilon + \mathcal{O}(\epsilon^2), \qquad u_3 = \frac{\epsilon}{w} + \mathcal{O}(\epsilon^2)\ .$$

While u_2 and u_3 only involve the Y function Y_2 in the fundamental strip, we need to use the recursion relation (3.10) to find u_1. Hence, all the three cross ratios indeed show their Regge behavior (2.28), (2.29) and (2.37).

4.2 Multi-Regge limit for $n = 7$ gluons

For the 7-point amplitude, the cross ratios are given in terms of the Y-functions as

$$u_{11} = \frac{Y^{[2]}_{2,2}}{1 + Y^{[2]}_{2,2}}, \qquad u_{21} = \frac{Y^{[-2]}_{2,2}}{1 + Y^{[-2]}_{2,2}}, \qquad u_{31} = \frac{Y^{[0]}_{2,2}}{1 + Y^{[0]}_{2,2}}, \tag{4.3}$$

$$u_{12} = \frac{Y^{[-3]}_{2,1}}{1 + Y^{[-3]}_{2,1}}, \qquad u_{22} = \frac{Y^{[-1]}_{2,1}}{1 + Y^{[-1]}_{2,1}}, \qquad u_{32} = \frac{Y^{[1]}_{2,1}}{1 + Y^{[1]}_{2,1}}. \tag{4.4}$$

We are going to demonstrate that that the cross ratios obtained from the Y-system for $n = 7$ display multi-Regge behavior if we take

$$\begin{aligned} m_s \to \infty \quad &, \quad C_s = \text{const.} \\ \phi_1 \to 0 \quad &, \quad \phi_2 \to -\frac{\pi}{4}\ . \end{aligned} \tag{4.5}$$

Note that the limiting value for the second angle ϕ_2 is non-vanishing. In the subsequent section we shall argue that in this limit, all integral contributions may be neglected and that the

prescription (4.5) is the only one that provides the correct Regge asymptotics of cross ratios. For the moment let us just check how things work with the limit we propose. As in the discussion for $n = 6$ we shall switch from variables m_s and ϕ_s to

$$\epsilon_1 = e^{-m_1 \cos\phi_1}, \qquad w_1 = e^{m_1 \sin\phi_1}, \tag{4.6}$$

$$\epsilon_2 = e^{-m_2 \cos\left(\frac{\pi}{4}+\phi_2\right)}, \qquad w_2 = e^{m_2 \sin\left(\frac{\pi}{4}+\phi_2\right)}. \tag{4.7}$$

In the above mentioned limit (4.5), these quantities behave as $\epsilon_i \to 0$, $w_i \to$ const. Let us begin our study of cross rations the simplest cases, namely the two cross ratios

$$u_{32} = \frac{Y_{2,1}^{[1]}}{1+Y_{2,1}^{[1]}} \cong \frac{e^{-\sqrt{2}m_1 \cos\left(\frac{\pi}{4}-\phi_1\right)}}{1+e^{-\sqrt{2}m_1 \cos\left(\frac{\pi}{4}-\phi_1\right)}} = \frac{\frac{\epsilon_1}{w_1}}{1+\frac{\epsilon_1}{w_1}} = \frac{\epsilon_1}{w_1} + \mathcal{O}(\epsilon^2), \tag{4.8}$$

$$u_{22} = \frac{Y_{2,1}^{[-1]}}{1+Y_{2,1}^{[-1]}} \cong \frac{e^{-\sqrt{2}m_1 \cos\left(\frac{\pi}{4}+\phi_1\right)}}{1+e^{-\sqrt{2}m_1 \cos\left(\frac{\pi}{4}+\phi_1\right)}} = \frac{\epsilon_1 w_1}{1+\epsilon_1 w_1} = \epsilon_1 w_1 + \mathcal{O}(\epsilon^2). \tag{4.9}$$

Up to this point, things work pretty much the same way as for the cross ratios u_2 and u_3 in the case of $n = 6$. The next cross ratio we want to look at is

$$u_{31} = \frac{Y_{2,2}^{[0]}}{1+Y_{2,2}^{[0]}} \cong \frac{e^{-\sqrt{2}m_2 \cos\phi_2}}{1+e^{-\sqrt{2}m_2 \cos\phi_2}} = \frac{\frac{\epsilon_2}{w_2}}{1+\frac{\epsilon_2}{w_2}} = \frac{\epsilon_2}{w_2} + \mathcal{O}(\epsilon^2) \tag{4.10}$$

which is the first one to contain ϕ_2. It is this last computation that suggests for the first time to set the limiting value of ϕ_2 to $\phi_2 = \pi/4$. If we had set $\phi_2 = 0$, for example, we would have been forced to omit the shifts by $\pi/4$ in the arguments of the trigonometric functions in eq. (4.7) in order to ensure finiteness of w_2. Without the shifts, the Regge limit of u_{31} would have been given by ϵ_2. But since the definition of w_2 and ϵ_2 included a shift, we had to add and subtract the limiting value $\pi/4$ of the angle ϕ_2 in the argument of the cosine. This is how we obtained the familiar looking Regge asymptotics of u_{31} even though the construction of the cross ratio only involved $Y_{2,2}^{[0]}$ with a vanishing upper index.
All remaining cross ratios involve values of Y-functions outside the fundamental strip so that we need to make repeated use of the recursion relation. We see that

$$Y_{2,2}^{[-2]} = \frac{1+Y_{2,1}^{[-1]}}{Y_{2,2}^{[0]}\left(1+\frac{1}{Y_{3,2}^{[-1]}}\right)\left(1+\frac{1}{Y_{1,2}^{[-1]}}\right)} \cong \frac{1+\epsilon_1 w_1}{\frac{\epsilon_2}{w_2}(1+\frac{e^{-C_2}}{\epsilon_2})(1+\frac{e^{C_2}}{\epsilon_2})} = \epsilon_2 w_2 + \mathcal{O}(\epsilon^2)$$

and therefore

$$u_{21} = \frac{Y_{2,2}^{[-2]}}{1+Y_{2,2}^{[-2]}} \cong \frac{\epsilon_2 w_2}{1+\epsilon_2 w_2} = \epsilon_2 w_2 + \mathcal{O}(\epsilon^2). \tag{4.11}$$

Analogously, we obtain

$$Y_{2,2}^{[2]} \cong \frac{1+\frac{\epsilon_1}{w_1}}{\frac{\epsilon_2}{w_2}\left(1+w_2 e^{-C_2}\right)\left(1+w_2 e^{C_2}\right)}, \tag{4.12}$$

from which we find that

$$u_{11} = \frac{Y^{[2]}_{2,2}}{1+Y^{[2]}_{2,2}} \cong 1 - \left(w_2 + \frac{1}{w_2} + 2\cosh C_2\right)\epsilon_2 + \mathcal{O}(\epsilon^2). \tag{4.13}$$

The last cross ratio we need is given in terms of $Y^{[-3]}_{2,1}$. The Y-functions appearing in the recursion relation are given below (without the full calculation).

$$Y^{[-2]}_{3,1} \cong \frac{1+e^{C_2}\epsilon_2}{e^{-C_1}\epsilon_1\left(1+\frac{1}{\epsilon_1 w_1}\right)}, \qquad Y^{[-2]}_{1,1} \cong \frac{1+e^{-C_2}\epsilon_2}{e^{C_1}\epsilon_1\left(1+\frac{1}{\epsilon_1 w_1}\right)}.$$

This then leads to

$$Y^{[-3]}_{2,1} = \frac{1+Y^{[-2]}_{2,2}}{Y^{[-1]}_{2,1}\left(1+\frac{1}{Y^{[-2]}_{3,1}}\right)\left(1+\frac{1}{Y^{[-2]}_{1,1}}\right)} \cong \frac{(1+\epsilon_2 w_2)}{\epsilon_1 w_1\left(1+\frac{e^{-C_1}\epsilon_1\left(1+\frac{1}{\epsilon_1 w_1}\right)}{1+e^{C_2}\epsilon_2}\right)\left(1+\frac{e^{C_1}\epsilon_1\left(1+\frac{1}{\epsilon_1 w_1}\right)}{1+e^{-C_2}\epsilon_2}\right)}$$

and finally

$$u_{12} = \frac{Y^{[-3]}_{2,1}}{1+Y^{[-3]}_{2,1}} \cong 1 - \left(w_1 + \frac{1}{w_1} + 2\cosh C_1\right)\epsilon_1 + \mathcal{O}(\epsilon^2). \tag{4.14}$$

This shows that the choice of parameters indeed gives the right limits for the cross ratios.

4.3 Finding the correct limit

Our analysis in the previous section was based on the claim that integral contributions to the NLIE can be neglected in the limit (4.5). Under this assumption we showed that our cross ratios display multi-Regge behavior. On the other hand we also suggested that the limit (4.5) was uniquely fixed by these requirements. Let us now discuss these claims in a bit more detail. It is clear from the relations (4.3) and (4.4) that for a cross ratio vanishing in the multi-Regge limit, the corresponding value of the Y-function has to vanish, as well. Values of Y-functions that appear in the cross ratios $u_{1\sigma}$, on the other hand, must diverge in the multi-Regge limit. For example, from the limiting behavior $u_{31} \to 0$ we conclude $Y^{[0]}_{2,2} \to 0$. Therefore, $\log Y^{[0]}_{2,2}$ has to be large and negative. The same follows for the value $\log Y^{[-1]}_{2,1}$ considering that $u_{32} \to 0$ in the multi-Regge limit. Because of the way the parameter m_s enters into eq. (3.3) we enforce the desired behavior if we make m_s very large. In this limit, the integrals appearing in eqs. (3.2)-(3.4) can be neglected because, assuming real masses for the moment, their leading contribution can be written schematically as

$$\int d\theta' K(\theta-\theta')\log\left(1+\mathrm{Y}(\theta')\right) \cong \int d\theta' K(\theta-\theta')\log\left(1+e^{-m_s\cosh\theta'}\right) \to 0, \tag{4.15}$$

as $m_s \to \infty$. This remains true even after introducing complex masses, as is shown in section 5.1. In this limit, we can now study the behaviour of the Y-functions and find constraints on the ϕ_s and C_s.

For further illustration we now wish to look at the cross ratios u_{11} and analyze how we ensure $u_{11} \to 1$ in the multi-Regge limit. The relevant value of the Y-function is given by

$$\mathrm{Y}^{[2]}_{2,2} \cong \frac{1+e^{-\sqrt{2}m_1\cos\left(\frac{\pi}{4}-\phi_1\right)}}{e^{-\sqrt{2}m_2\cos\phi_2}\left(1+e^{m_2\cos\left(\frac{\pi}{4}-\phi_2\right)-C_2}\right)\left(1+e^{m_2\cos\left(\frac{\pi}{4}-\phi_2\right)+C_2}\right)} \to \infty. \tag{4.16}$$

If we want the Y-function to diverge, every term of the denominator has to vanish in the multi-Regge limit. Writing the denominator as

$$e^{-\sqrt{2}m_2\cos\phi_2} + e^{\sqrt{2}m_2\sin\phi_2} + 2\cosh C_2 e^{-m_2\cos\left(\frac{\pi}{4}+\phi_2\right)} \tag{4.17}$$

we see that

$$\phi_2 \in \left(-\frac{\pi}{2},\frac{\pi}{2}\right) \cap (-\pi,0) \cap \left(-\frac{3\pi}{4},\frac{\pi}{4}\right) = \left(-\frac{\pi}{2},0\right), \tag{4.18}$$

at least if we assume that it will stay in the interval between $-\pi \leq \phi_2 \leq \pi$. In order to find the specific value that ϕ_2 should assume, we recall from eq. (2.30) that the ratio u_{21}/u_{31} must remain constant in the multi-Regge limit. According to our equations (4.3), this requires

$$\frac{Y^{[-2]}_{2,2}}{Y^{[0]}_{2,2}} \cong \frac{1}{e^{-2\sqrt{2}m_2\cos\phi_2}\left(1+e^{m_2\cos\left(\frac{\pi}{4}+\phi_2\right)-C_2}\right)\left(1+e^{m_2\cos\left(\frac{\pi}{4}+\phi_2\right)+C_2}\right)} \to \text{const.} \tag{4.19}$$

Here we have also used that both $Y^{[-2]}_{2,2}$ and $Y^{[0]}_{2,2}$ vanish in the multi-Regge limit. For the ratio of these values to be constant, at least one term of the denominator has to go to a constant with the other terms in the denominator going to zero. This suggests the two possible limits $\phi_2 \to -\frac{\pi}{4}$ or $\phi_2 \to \frac{\pi}{2}$. The latter limiting behavior, however, is excluded by the constraint we derived from $u_{11} \to 1$. A similar analysis is carried out for the remaining Y-functions in appendix A. There we derive all constraints one can put on the parameters of the NLIE. These are solved by $\phi_1 \to 0$ and $\phi_2 \to -\frac{\pi}{4}$, as we anticipated above. And indeed in section 4 we saw that such a limiting behavior of the phases ϕ_s produces the correct multi-Regge behavior for all the cross ratios.

The most surprising outcome of our discussion for $n = 7$ is that the limiting values of the phases need no longer be zero, in contrast to what we found for $n = 6$. One may generalize the arguments outlined here to larger number of gluons $n \geq 8$ to find that $\phi_s = -(s-1)\frac{\pi}{4}$ appear to be the correct values for the phases in the multi-Regge limit. A full proof of this fact, however, requires a closer look at the Y-system for non-zero phases and possible residues.

5 Multi-Regge limit of the TBA - general case

As we have argued in the previous section, the phases ϕ_s may approach large values in the multi-Regge regime. Since the original Y-system is only valid as long as phases satisfy $|\phi_s - \phi_{s'}| < \pi/4$ we must be prepared to include additional contributions that arise from poles in the kernel, see

our comments in section 3.1 and [30]. In the following analysis we will make the ansatz

$$m_s \to \infty, \tag{5.1}$$

$$\phi_s = -(s-1)\frac{\pi}{4}, \tag{5.2}$$

$$C_s = \text{const.} \tag{5.3}$$

for the multi-Regge limit of the parameters m_s, ϕ_s and C_s. Our main goal is to show that in this limit, the cross ratios (2.6)-(2.8) have multi-Regge behavior, i.e. that they behave as described in eqs. (2.28), (2.29) and (2.37). The contributions from poles of the kernel functions turn out to play a vital role in this analysis. Therefore, we begin with a few general comments on the behavior of the Y-system for large masses in the presence of large phases ϕ_s. These then allow us to find explicit values for the physical cross ratios for an arbitrary number of external gluons.

5.1 Large phase residues and multi-Regge limit

In this section we revisit the structure of the Y-system equations in the presence of large phases ϕ_s. Recall that in the presence of complex masses the equations can be written as

$$\log\tilde{\mathrm{Y}}_{2,s}(\theta) = -\sqrt{2}|m_s|\cosh\theta + \sum_{a',s'}\int d\theta' K^{2,a'}_{s,s'}(\theta-\theta'+i\phi_s - i\phi_{s'})\log(1+\tilde{\mathrm{Y}}_{a',s'}(\theta')), \tag{5.4}$$

where $\tilde{\mathrm{Y}}_{a,s}(\theta) = \mathrm{Y}_{a,s}(\theta+i\phi_s)$, cf. [23]. We only displayed the equations for $\tilde{\mathrm{Y}}_{2,s}$ here, but similar equations obviously hold for the other Y-functions, as well. Eqs. (5.4) determine the functions $\tilde{\mathrm{Y}}$ in the fundamental strip $|\mathrm{Im}\theta| < \pi/4$ as long as the phase differences satisfy $|\phi_s - \phi_{s'}| < \pi/4$. For $\mathrm{Im}(\theta + i\phi_s - i\phi_{s'}) = k\cdot\frac{\pi}{4}$, the kernels are singular and we have to pick up residues from these poles[2]. More precisely, the kernels K_2, K_3 become singular for $k = 2n+1$, while K_1 is singular for $k = 2(2n+1)$. In other words, at least one of the kernel functions has a pole whenever

$$k \in \mathcal{X} := \{2\mathbb{Z}+1\} \cup \{2(2\mathbb{Z}+1)\} \ .$$

Once we include the residues of the pole contributions, the integral equations are given by

$$\begin{aligned}\log\tilde{\mathrm{Y}}_{2,s}(\theta) = -\sqrt{2}|m_s|\cosh\theta &+ \sum_{\nu} n_\nu \log\left(1+\tilde{\mathrm{Y}}_{a_\nu,s_\nu}\left(\theta+i\phi_s - i\phi_{s_\nu} - ik_\nu\frac{\pi}{4}\right)\right) \\ &+ \sum_{a',s'}\int d\theta' K^{2,a'}_{s,s'}(\theta-\theta'+i\phi_s - i\phi_{s'})\log(1+\tilde{\mathrm{Y}}_{a',s'}\left(\theta'\right))\end{aligned} \tag{5.5}$$

In eq. (5.5), it is understood that the sum in the first line extends over all the relevant pole contributions. We will discuss this in more detail below. As they stand, equations (5.5) are valid for arbitrary θ in the complex plane. Of course, the number of terms in the summation over ν depends on the value of $\mathrm{Im}(\theta)$.

Before we proceed to analyze the behavior of eqs. (5.5) in the limit of large masses, let us have

[2] Note that we have to pick up a pole only if the kernel singularity is crossed. For values on the singularities, an $i0$-prescription can be used (cf.[23]).

a closer look at the Y-system for real argument θ. Recall from section 3.1 that the kernels $K_{s,s'}^{a,a'}$ are non-zero only for $s' = s$ or $s' = s \pm 1$. Hence, the differences $\phi_s - \phi_{s'}$ that appear in our limit (5.2) are restricted to values $|\phi_s - \phi_{s'}| \leq \pi/4$. We conclude that, as long as θ is real, no poles of the kernel functions are actually crossed in the limit (5.2) and hence the Y-functions $\mathrm{Y}_{a,s}(\theta), \theta \in \mathbb{R}$, obey the original Y-system without additional residue terms.
This comment becomes important in passing to the large mass limit of eqs. (5.5). Note that the integral in the second line extends over θ' along the real line. Hence, to evaluate the integral, we only need to know $\tilde{\mathrm{Y}}_{a',s'}(\theta')$ for real θ' where it is unaltered by pole contributions and consequently still given by

$$\tilde{\mathrm{Y}}_{2,s'}(\theta') \cong e^{-\sqrt{2}|m_s|\cosh\theta'} \quad , \quad \tilde{\mathrm{Y}}_{a',s'}(\theta') \cong e^{-|m_s|\cosh\theta' + (a'-2)C_s} \quad \text{for } a' = 1, 3,$$

in the limit of large masses $|m_s|$ and for $\theta' \in \mathbb{R}$. It follows once again that all integral contributions to eqs. (5.5) can be neglected in the limit (5.2). Shifting back to the Y-functions, we see that after neglecting the integrals the equations look like[3]

$$\log \mathrm{Y}_{2,s}(\theta) = -\sqrt{2}|m_s|\cosh(\theta - i\phi_s) + \sum_\nu n_\nu \log\left(1 + \mathrm{Y}_{a_\nu,s_\nu}\left(\theta - ik_\nu\frac{\pi}{4}\right)\right). \tag{5.6}$$

It is important now to describe the sum over pole contributions in some more detail. To begin with all labels a_ν, s_ν can only run over nine possible values. While a_ν is free to assume any of its three values, s_ν cannot deviate from s by more than one unit, i.e.

$$a_\nu = 1, 2, 3 \quad , \quad s_\nu \in \{s, s \pm 1\} .$$

Given any such choice of (a_ν, s_ν) we compute the quantity $\kappa_{s_\nu} = \frac{4}{\pi}\mathrm{Im}(\theta - i\phi_{s_\nu})$. It determines the possible values of the integer

$$k_\nu \ \in \ (0, \kappa_{s_\nu}) \cap \mathcal{X} .$$

Given (a_ν, s_ν) and k_ν we must still find the integer n_ν. It is determined by the form of the functions α_s, β_s and γ_s in eqs. (3.6)-(3.8), the coefficients of these functions in the Y-system (3.2)-(3.4) and sign of k_ν. We will discuss some examples in the next subsection.

5.2 Multi-Regge limit for $n = 8$ gluons

As we shall discuss at the end of the next subsection, pole contributions from the kernels only start to enter the limit (5.2) starting from $n = 8$ external gluons. It is useful to analyze the $n = 8$ case first to illustrate the general formula (5.6). Generalizing the variables we used in our analysis of the multi-Regge limit for 7 gluons we introduce

$$\epsilon_s = e^{-m_s\cos\left((s-1)\frac{\pi}{4}+\phi_s\right)}, \tag{5.7}$$

$$w_s = e^{m_s\sin\left((s-1)\frac{\pi}{4}+\phi_s\right)}, \tag{5.8}$$

where $s = 1, 2, 3$. In the limit (5.2) these variables behave as $\epsilon_s \to 0$ and $w_s \to$ const.
As an example, let us analyze the limit of $Y_{2,2}^{[-2]}$. Since we want to determine $\mathrm{Y}_{2,2}$ at $\theta = -i\pi/2$

[3] Note that the variable θ was shifted by $-i\phi_s$ when we passed from $\tilde{\mathrm{Y}}_{a,s}$ to $\mathrm{Y}_{a,s}$.

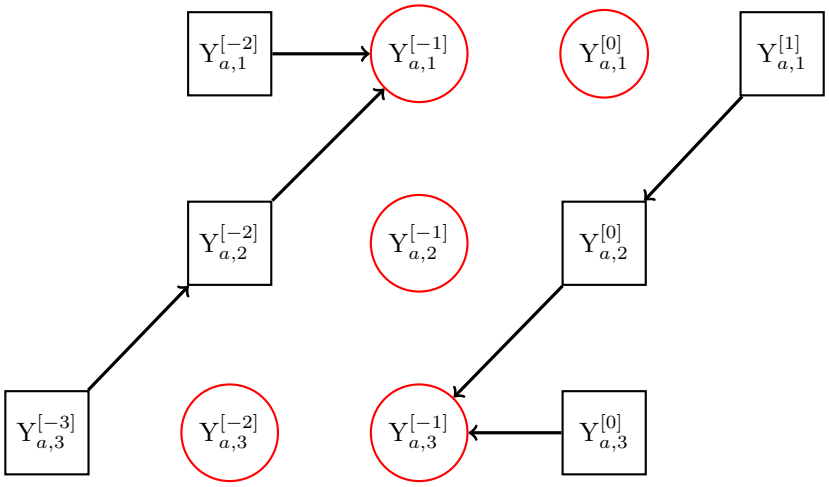

Figure 3. Residue structure for Y-functions in 8-point case.

and $\phi_{s_\nu} = -(s_\nu - 1)\pi/4$, the parameter κ_{s_ν} defined at the end of the previous subsection reads $\kappa_{s_\nu} = s_\nu - 3$. In order for the interval $(0, s_\nu - 3)$ to have a non-vanishing intersection with $\mathcal{X}$, we must have $s_\nu = 1$. In the case at hand, the intersection consists of a single point $k = -1$. Looking back at eq. (3.3) we note that only K_2 possesses a pole at $-i\pi/4$. The coefficient of K_2 in the equation for $\log \mathrm{Y}_{2,2}$ is $-\alpha_2$. The latter contains only one contribution with $1 = s_\nu = s-1$, namely the term $-\log(1 + \mathrm{Y}_{2,1})$. Consequently, we find

$$Y^{[-2]}_{2,2} = e^{-\sqrt{2}m_2 \cos(\pi/2+\phi_2)} \cdot \left(1 + Y^{[-1]}_{2,1}\right) = \epsilon_2 w_2 \cdot \left(1 + Y^{[-1]}_{2,1}\right). \tag{5.9}$$

Note that in this particular case the correction term becomes trivial in the limit (5.2) since $Y^{[-1]}_{2,1} = \exp(-m_s)$. Analogously, we can analyze the residue structure of the remaining Y-functions. The result is shown in figure 3 which we explain in the following. Every node in the diagram represents the 3 values $\mathrm{Y}^{[k]}_{as}$ with $a = 1, 2, 3$ while s and k are kept fixed. Encircled nodes correspond to Y-functions that receive no corrections from residues. Arrows points to the nodes from which a given Y-function receives residue terms. Our result (5.9), for example, is represented by the arrow that connects the square box around $\mathrm{Y}^{[-2]}_{a,2}$ with the circle around $\mathrm{Y}^{[-1]}_{a,1}$. Values of $\mathrm{Y}^{[r]}_{a,s}$ that are not included in the figure not only receive residues with $k_\nu = \pm 1$, but include higher values of k_ν. Those have a more complicated structure and are better bypassed through the use of recursion relations, if possible. We see that with the help of the Y-functions at $\theta = -i\pi/4$ we can determine all Y-functions at $\theta = 0$. Once we have constructed $\mathrm{Y}^{[-1]}_{a,s}$ and $\mathrm{Y}^{[0]}_{a,s}$, all remaining values can be reconstructed with the help of the recursion relation (3.10). A complete analysis gives the following results for the cross ratios in the limit (5.2),

$$u_{1\sigma} = 1 - \left(w_{n-4-\sigma} + \frac{1}{w_{n-4-\sigma}} + 2\cosh C_{n-4-\sigma}\right)\epsilon_{n-4-\sigma}, \tag{5.10}$$

$$u_{2\sigma} = \epsilon_{n-4-\sigma} w_{n-4-\sigma}, \tag{5.11}$$

$$u_{3\sigma} = \epsilon_{n-4-\sigma} w^{-1}_{n-4-\sigma}. \tag{5.12}$$

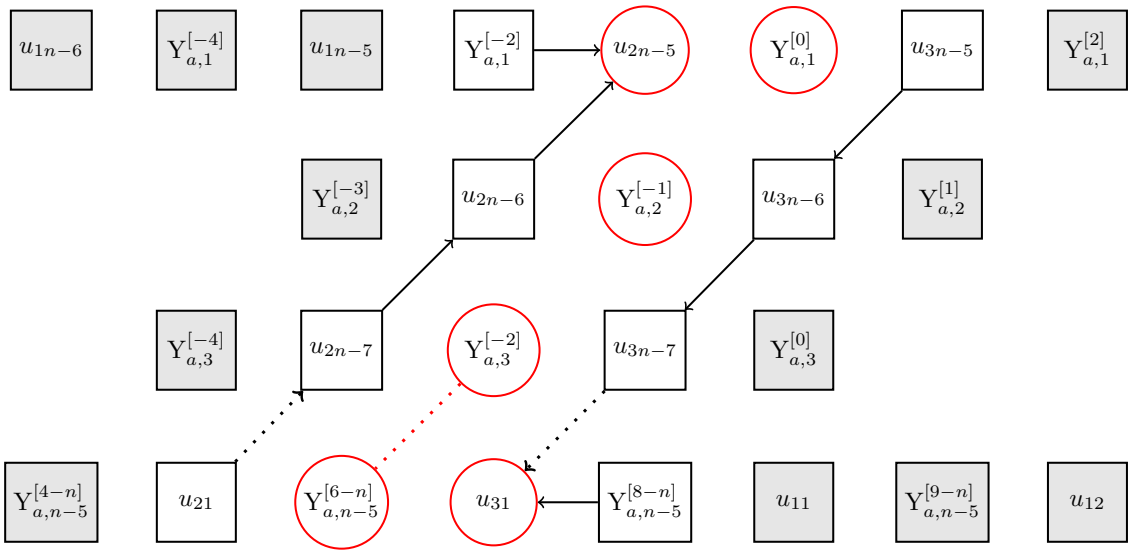

Figure 4. Residue structure for n points. Y-functions not shown in the figure correspond to gray boxes.

So, we find that all cross ratios have multi-Regge asymptotics (2.28), (2.29) and (2.37).

5.3 The general case of n-gluon scattering

After discussing 7- and 8-gluon amplitudes we finally proceed to the general case. Our goal is to show that the cross ratios (2.6)-(2.8) that are obtained from the Y-functions through eqs. (3.16) show multi-Regge behaviour (2.28), (2.29) and (2.37) in the limit (5.2). As before, we can study the residue structure of the Y-system for phases $\phi_s = -(s-1)\pi/4$. The results are encoded in figure 4. Gray nodes correspond to Y-functions with a more complicated residue structure. We explain in appendix B how our pattern can be used to read off the resulting contributions. If a cross ratio (3.16) is obtained from the Y-function $Y^{[k]}_{2,s}$, we have indicated this by putting the cross ratio into the node instead of the Y-function. We have already used the shift symmetry to put some of the $u_{1\sigma}$ in the first row.
We see that the cross ratios $u_{2\sigma}$ and $u_{3\sigma}$ lie on a diagonal whose '*residue flow*' stays within the diagonal. The endpoints of the residue flow are given by u_{31} and $u_{2\,n-5}$, which are free of residues and can be calculated directly to to give

$$u_{31} = \epsilon_{n-5} w^{-1}_{n-5}, \tag{5.13}$$

$$u_{2\,n-5} = \epsilon_1 w_1. \tag{5.14}$$

It is not difficult to determine the remaining cross ratios $u_{2\sigma}$ and $u_{3\sigma}$. Recall from eq. (3.16) that the cross ratios $u_{2\sigma}$ are given by

$$u_{2\sigma} = \frac{Y^{[-(n-4-\sigma)]}_{2,n-4-\sigma}}{1 + Y^{[-(n-4-\sigma)]}_{2,n-4-\sigma}}. \tag{5.15}$$

According to our general expression (5.6), the values of the Y-functions that enter these cross ratios are given by

$$Y_{2,s}^{[-s]} = e^{-\sqrt{2}m_s \cos\left(\frac{\pi}{4}+(s-1)\frac{\pi}{4}+\phi_s\right)} \cdot (\text{Residue terms}) = \epsilon_s w_s \cdot (\text{Residue terms}) \,. \tag{5.16}$$

We can conclude by iteration that the residue terms along this diagonal only introduce corrections of the order ϵ^2 or higher and can be neglected. Hence, we obtain

$$u_{2\sigma} = \epsilon_{n-4-\sigma} w_{n-4-\sigma} \,. \tag{5.17}$$

One can go through the same arguments to find

$$u_{3\sigma} = \epsilon_{n-4-\sigma} w_{n-4-\sigma}^{-1} \,. \tag{5.18}$$

This finally leaves us with the cross ratios $u_{1\sigma}$ for which we have to work a little bit harder, as these variables all have a more complicated residue structure. We will make use of an inductive argument. Going from a n-point amplitude to a $(n+1)$-point amplitude introduces another row in our above pattern. However, the old Y-functions do not change their values as long as their residues are not affected by the new row. What changes, however, is the location of the cross ratios in the pattern. The most important change for our purposes is that all $u_{1\sigma}$ in the first row are shifted by two boxes to the left in our pattern, and a new cross ratio $u_{1((n+1)-5)}$ appears which is related to $\mathrm{Y}_{2,1}^{[-3]}$. This means, for example, that $u_{1((n+1)-5)}$ in the $(n+1)$-point amplitude will take the value of u_{1n-5} in the n-point amplitude, since all residue are unaffected by the new row. Following our discussion in appendix B, it is clear that a Y-function will keep its n-point value if the diagonal from its node to the lower right hits the $(n+1)$-point $u_{2\sigma}$-diagonal at the position of u_{22}, or above. It turns out that the last element, i.e. the element with smallest value of θ, in the first row that keeps its value is given by u_{13}. This means, that all $u_{1\sigma}$ for $\sigma = 3, ..., n-4$ can be calculated using the known n-point values. However, u_{11} and u_{12} are then given by the symmetry (3.18) relating $u_{1\sigma} \leftrightarrow u_{1(n-4-\sigma)}$. We have established above that

$$u_{1\sigma} = 1 - \left(w_{n-4-\sigma} + \frac{1}{w_{n-4-\sigma}} + 2\cosh C_{n-4-\sigma} \right) \epsilon_{n-4-\sigma} \tag{5.19}$$

for the 7- and 8-point amplitude. By the previous argument, the same remains true for all values of n. This shows that the n-point solution is a $(n-5)$-fold copy of the 6 point solution. In conclusion, we now confirmed our identification of the multi-Regge regime with the limit (5.2) of the parameters in the Y-system.

5.4 The 7-point case revisited

In the light of the general result derived in the last section, let us revisit the 7-point case to study explicitly the equations governing the Y-system in the fundamental strip and to understand why no large residues had to be considered in our earlier analysis. Recall that for 7-points the multi-Regge limit corresponds to taking m_s large, C_s constant, $\phi_1 = 0$ and $\phi_2 = -\pi/4$. For $-\pi/4 < \mathrm{Im}\theta \leq 0$ we have that $\mathrm{Im}\,(\theta - i\phi_s) \in (-\pi/4, \pi/4)$. Since none of these terms crosses a multiple of $\pi/4$, no singularities arise and we do not have to pick up any residues. Therefore, the Y-system (5.4) is valid without any modifications. For $0 < \mathrm{Im}\theta < \pi/4$, however, $\mathrm{Im}\,(\theta - i\phi_2)$

crosses $\pi/4$ and we have to pick up residues. Following the procedure outlined in the previous subsection, we find the following equations:

$$\begin{aligned}
\log \mathrm{Y}_{11}(\theta) =& -|m_1|\cosh(\theta - i\phi_1) + \sum_{a',s'} \int d\theta' K_{1,s'}^{1,a'}\left(\theta - \theta' - i\phi_{s'}\right) \log\left(1 + \mathrm{Y}_{a',s'}\left(\theta' + i\phi_{s'}\right)\right) \\
& - C_1 + \log\left(1 + \mathrm{Y}_{12}\left(\theta - i\frac{\pi}{4}\right)\right), \\
\log \mathrm{Y}_{21}(\theta) =& -\sqrt{2}|m_1|\cosh(\theta - i\phi_1) + \sum_{a',s'} \int d\theta' K_{1,s'}^{2,a'}\left(\theta - \theta' - i\phi_{s'}\right) \log\left(1 + \mathrm{Y}_{a',s'}\left(\theta' + i\phi_{s'}\right)\right) \\
& + \log\left(1 + \mathrm{Y}_{22}\left(\theta - i\frac{\pi}{4}\right)\right), \\
\log \mathrm{Y}_{31}(\theta) =& -|m_1|\cosh(\theta - i\phi_1) + \sum_{a',s'} \int d\theta' K_{1,s'}^{3,a'}\left(\theta - \theta' - i\phi_{s'}\right) \log\left(1 + \mathrm{Y}_{a',s'}\left(\theta' + i\phi_{s'}\right)\right) \\
& + C_1 + \log\left(1 + \mathrm{Y}_{32}\left(\theta - i\frac{\pi}{4}\right)\right), \\
\log \mathrm{Y}_{12}(\theta) =& -|m_2|\cosh(\theta - i\phi_2) + \sum_{a',s'} \int d\theta' K_{2,s'}^{1,a'}\left(\theta - \theta' - i\phi_{s'}\right) \log\left(1 + \mathrm{Y}_{a',s'}\left(\theta' + i\phi_{s'}\right)\right) \\
& - C_2 - \log\left(1 + \mathrm{Y}_{22}\left(\theta - i\frac{\pi}{4}\right)\right), \\
\log \mathrm{Y}_{22}(\theta) =& -\sqrt{2}|m_2|\cosh(\theta - i\phi_2) + \sum_{a',s'} \int d\theta' K_{2,s'}^{2,a'}\left(\theta - \theta' - i\phi_{s'}\right) \log\left(1 + \mathrm{Y}_{a',s'}\left(\theta' + i\phi_{s'}\right)\right) \\
& - \log\left(1 + \mathrm{Y}_{12}\left(\theta - i\frac{\pi}{4}\right)\right) - \log\left(1 + \mathrm{Y}_{32}\left(\theta - i\frac{\pi}{4}\right)\right), \\
\log \mathrm{Y}_{32}(\theta) =& -|m_2|\cosh(\theta - i\phi_2) + \sum_{a',s'} \int d\theta' K_{2,s'}^{3,a'}\left(\theta - \theta' - i\phi_{s'}\right) \log\left(1 + \mathrm{Y}_{a',s'}\left(\theta' + i\phi_{s'}\right)\right) \\
& + C_2 - \log\left(1 + \mathrm{Y}_{22}\left(\theta - i\frac{\pi}{4}\right)\right).
\end{aligned}$$

Let us now examine the Y-functions appearing in the residue terms. To be specific, we will focus on the term involving $\mathrm{Y}_{12}(\theta - i\pi/4)$ in the first equation. For the argument of this Y-function we have $-\pi/4 < \mathrm{Im}(\theta - i\pi/4) < 0$. As argued before, in this range of the argument no residue terms appear and in the multi-Regge limit the Y-function is given by

$$\mathrm{Y}_{12}\left(\theta - i\frac{\pi}{4}\right) \cong e^{-|m_2|\cosh\left(\theta - i\frac{\pi}{4} - i\phi_2\right) - C_2} = e^{-C_2} \epsilon_2^{\cosh\theta} w_2^{i\sinh\theta}. \tag{5.20}$$

The exponent of ϵ_2 is positive in the chosen range of θ. Therefore, the function goes to zero in the multi-Regge limit and the residue containing Y_{12} gives a negligible contribution. Analogously, we can analyze the remaining residue terms. It turns out that they are all negligible. The same is actually true for $n = 8$ external gluons. However, starting from 9-points the residue terms give significant contributions in the fundamental strip, see Appendix C for explicit expressions.

6 Bethe ansatz

The analysis outlined above has shown that the non-linear integral equations that control the n-gluon amplitudes at strong coupling simplify drastically when we take the multi-Regge limit. In the limiting regime we can actually neglect the integral contributions, possibly after taking some residue terms into account. Such a limit is well known in the theory of integrable systems. It corresponds to a large volume limit in which the solution of the integrable model boils down to solving a set of algebraic Bethe ansatz equations.

Before we recall how the Bethe ansatz equations emerge in the multi-Regge limit, we need to comment a bit more on the residue terms we picked up while sending the phases ϕ_s to their limiting values $\psi_s = (1-s)\pi/4$. The appearance of such residue terms has been discussed for the AdS_3 Y-system in Appendix B of [23]. Using experience from closely related wall-crossing phenomena (see [36]), the authors of [23] demonstrated how residue terms can be absorbed in a redefinition of the Y-functions. While bringing the equations back into the standard form of a Y-system,

$$-\log \tilde{\mathrm{Y}}_A(\theta) = p_A(\theta) + \sum_B \int \frac{d\theta'}{2\pi} K_{AB}(\theta-\theta') \log\left(1+\tilde{\mathrm{Y}}_B(\theta')\right) \quad , \tag{6.1}$$

it is necessary to introduce additional Y-functions. This implies that the new set of equations (6.1) might involve more than the $3n-15$ Y-functions we started with. The complete set of Y-functions is enumerated by the label $A, B, \ldots$. Constructing the source terms p_A and the kernel functions K_{AB} is part of the task one has to address while passing from a modified Y-system with residue terms back to a Y-system of the form (6.1). We defer a detailed discussion of this procedure for the AdS_5 Y-system at $\phi_s = (1-s)\pi/4$ to a future publication. Let us only mention that the source terms p_A for the new Y-functions that are introduced while rewriting the equations possess the canonical form with masses m_A that can be obtained from the $n-5$ masses m_s of the original Y-system.

Once we accept that the original Y-system with large phases $\phi_s = (1-s)\pi/4$ can be brought into the form (6.1), we are prepared to review how Bethe ansatz equations emerge. In order to do so, we represent the kernel functions K_{AB} through new objects S_{AB},

$$K_{AB}(\theta) = -\partial_\theta \log S_{AB}(\theta) \quad . \tag{6.2}$$

As observed first by Dorey and Tateo [25, 26], upon analytic continuation of the parameters some of the solutions to the equations $\tilde{\mathrm{Y}}_A(\theta) = -1$ may cross the real axis. We shall enumerate those solutions by an index $\nu = 1, \ldots, N_A$:

$$\tilde{\mathrm{Y}}_A(\theta_\nu^{(A)}) = -1, \quad \text{for} \quad \nu = 1, \ldots, N_A \quad . \tag{6.3}$$

When this happens, the integral on the right-hand side of equation (6.1) picks up a residue term since there is a pole crossing the integration contour. Hence, after analytic continuation

the equations (6.1) take the form

$$-\log \tilde{\mathrm{Y}}_A(\theta) = p_A(\theta) + \sum_B \sum_{\nu=1}^{N_B} \log S_{AB}(\theta - \theta_\nu^{(B)}) + \sum_B \int \frac{d\theta'}{2\pi} K_{AB}(\theta - \theta') \log\left(1 + \tilde{\mathrm{Y}}_B(\theta')\right) \quad . \tag{6.4}$$

If we now send the parameters of our nonlinear integral equations back into a regime where the integrals can be neglected, e.g. into the multi-Regge regime we explored in this note, the equations (6.4) become

$$-\log \tilde{\mathrm{Y}}_A(\theta) = p_A(\theta) + \sum_B \sum_{\nu=1}^{N_B} \log S_{AB}(\theta - \theta_\nu^{(B)}) \quad . \tag{6.5}$$

We can exponentiate this set of equations for the functions $\mathrm{Y}_A(\theta)$ and insert the values $\theta = \theta_\nu^{(A)}$ satisfying eq. (6.3) to obtain

$$e^{iRk_A(\theta_\mu^{(A)})} = \prod_B \prod_{\nu=1}^{N_B} S_{AB}(\theta_\mu^{(A)} - \theta_\nu^{(B)}) \tag{6.6}$$

with $k_A(\theta) := ip_A(\theta)/R$. The parameter R and the functions k_A were introduced here to help interpreting the equations (6.6). In our context, these equations simply determine the possible location of the solutions $\theta_\nu^{(A)}$ to the equations (6.3). But the form of the equations coincides with the usual Bethe ansatz that imposes single-valuedness of wave functions for particles on a 1-dimensional circle of circumference R. The term $\exp(iRk_A)$ accounts for the phase shift of a freely moving particle with momentum $k_A(\theta_\nu^{(A)})$ when we take it once around the circle. The remaining factors arise from the scattering with other particles that may be distributed along the 1-dimensional circle. Hence, the quantities S_{AB} introduced in eq. (6.2) are interpreted as a scattering matrix for excitations of some integrable system and the source terms k_A describe the momentum.

To make the Bethe ansatz equations (6.6) for the multi-Regge limit of the bubble ansatz more explicit, we need to determine the range of the label A, the source terms $p_A(\theta)$ and the kernel functions $K_{AB}(\theta)$, or rather the corresponding S-matrices. Only in the case of $n = 6$ external gluons these can be read off easily from the original Y-system. The general case will be addressed in a future publication. Much of the above would have remained valid if we had not brought to the modified Y-system back into the form (6.1). But the resulting Bethe ansatz equations (6.6) would have been modified as well, with the left hand side being replaced by a sum of products of 'phases' $\exp(iRk_{a,s})$. Examples can be worked out from our formulas for the multi-Regge limit of the Y-system with $n = 9$, see appendix C. Such modified Bethe ansatz equations can certainly be studied numerically. Nevertheless, we believe that a deeper understanding of the underlying integrable system requires to absorb the residue terms so that the Bethe ansatz equations take the standard form.

Let us finally discuss the form of the free energy (3.12). As explained in [23] the original expression remains valid in the presence of large phases ϕ_s, but it needs to be rewritten in

terms of the Y-functions $\tilde{\mathrm{Y}}_A$. Upon analytic continuation of the parameters, the Y-functions can give rise to pole terms that cross the real axis. This happens precisely when the conditions (6.3) are satisfied. After taking the multi-Regge limit, only these pole terms survive and one should obtain an expression of the form

$$A_{\text{free}} = \sum_A \sum_{\nu=1}^{N_A} e_A(\theta_\nu^{(A)}) \ . \tag{6.7}$$

with some energy functions $e_A = e_A(\theta)$ that must be determined while passing from the modified Y-system with residue terms to eqs. (6.1). Hence, in order to evaluate scattering amplitudes of strongly coupled $\mathcal{N} = 4$ SYM theory in the multi-Regge limit, we have to solve the Bethe ansatz equations (6.6) for the positions $\theta_\nu^{(A)}$ of the solutions to eq. (6.3). Once these are found, we can easily evaluate A_{free}.

7 Conclusions and outlook

In this note we studied the multi-Regge limit of scattering amplitudes in strongly coupled $\mathcal{N} = 4$ SYM theory for any number n of external gluons. As reviewed above, the remainder function $R^{(n)}$ is determined through an auxiliary 1D quantum system (3.2)-(3.4) which depends on $3n-15$ parameters m_s, ϕ_s and C_s. The latter map in a complicated way to the $3n-15$ independent cross ratios that parametrize the scattering process. Our central result (5.2) identifies the values of the parameters in the 1D quantum system that correspond to the multi-Regge limit of the 4-dimensional gauge theory. Since the relevant limit (5.2) involves sending all the mass parameters m_s to infinity, the multi-Regge (high-energy) regime of the gauge theory maps to the large volume (low energy) limit of the 1D quantum system. In such a limit, the 1D quantum system simplifies drastically. More precisely, the non-linear integral equations (3.2)-(3.4) can be replaced by a much simpler set of algebraic equations (6.6).

We find it remarkable that the computation of scattering amplitudes simplifies at both weak and strong coupling. In the quest for the exact S-matrix of $\mathcal{N} = 4$ SYM theory, one that interpolates all the way from weak to strong coupling, it could therefore pay off to consider the multi-Regge regime as an intermediate step before addressing general kinematics. Our results suggests that the multi-Regge regime could be tractable even for finite coupling, at least more tractable than the full dependence of the remainder functions on all the $3n-15$ cross ratios. On the other hand, the Regge-limit imposes very strong constrains on the analytical structure of the remainder functions $R^{(n)}$. Explicit formulas for the Regge-limit of the remainder functions could therefore be an important ingredient in reconstructing the full scattering amplitude from more basic data.

But before thinking about the interpolation to finite coupling, there are a few more immediate issues to be addressed. One is related to wall-crossing phenomena we briefly mentioned in section 6. Recall that our limit (5.2) involves large phases ϕ_s in which differences $|\phi_s - \phi_{s\pm1}|$ assume the critical value $\pi/4$. As we described in much detail, these large phases bring additional residue terms into the non-linear integral equations of the Y-system. This happens starting from $n = 7$ external gluons. The corresponding modified equations can be obtained through an algorithm we outlined in section 5.3. The simplest non-trivial example was spelled out

explicitly in subsection 5.4. Following a procedure that is inspired by the study of wall-crossing phenomena [36, 37], it should be possible to bring the modified Y-system into the standard form (6.1). Our discussion in section 6 assumed that the necessary steps have been carried out already. But in order to determine the precise range of the labels A, B, the momenta $p_A(\theta)$ and the S-matrix elements S_{AB} that enter eq. (6.6) for $n > 6$ external gluons, one cannot avoid a detailed analysis. We leave this to future research.
Finally, we need to establish a map between the analytic continuation of the kinematic variables and the numbers N^A of Bethe roots $\theta_\nu^{(A)}$ in the previous section. In the case of the hexagon, such a correspondence was determined through numerical studies. The authors of [24] found that the analytical continuation from the so-called physical to the mixed regime (see [24] for precise definitions) makes two solutions of eq. (6.3) cross the real axis. Hence, the multi-Regge limit of the $n = 6$ amplitude in the mixed regime corresponds to the energy of a doubly excited state in the 1D quantum system at infinite volume R. This agrees nicely with the analysis in the weakly coupled theory. For the Regge-limit of the full 2-loop hexagon remainder function $R^{(6)}$ to be non-zero, one needs to pass into the same mixed regime that is associated with a non-trivial doubly excited state of the Bethe ansatz equation (6.6). It is clearly desirable to extend such studies beyond the case of the hexagon. Note that for larger number of external gluons there exist many different regimes with non-vanishing Regge-limit which probe eigenvalues of the BKP Hamiltonian [38] with increasing number of sites [39]. We expect that such different regimes are associated with solutions of eqs. (6.6) with an increasing number N^A of Bethe roots.

Acknowledgments: We wish to thank Patrick Dorey, Nicolay Gromov, Paul Heslop, Andrey Kormilitzin, Jan Kotanski, Lev Lipatov, Jörg Teschner, Pedro Vieira and Gang Yang for valuable discussions. This work was supported in part by the SFB 676.

A Explicit values of Y-functions for 7-point amplitude

This appendix contains the complete analysis of the restrictions that the desired multi-Regge behavior of cross ratios imposes on the limiting values of the angles ϕ_s for $n = 7$ gluons. Some part of the required analysis was included and explained in section 4.3. Here we simply state the remaining set of formulas without further comments. Let us begin with the simplest cross ratios whose evaluation does not require any use of the recursion relation (3.10):

$$u_{31} \to 0 \implies Y_{2,2}^{[0]} \cong e^{-\sqrt{2}m_2 \cos\phi_2} \to 0 \qquad \Rightarrow \boxed{\phi_2 \in \left(-\frac{\pi}{2}, \frac{\pi}{2}\right)}$$

$$u_{32} \to 0 \implies Y_{2,1}^{[1]} \cong e^{-\sqrt{2}m_1 \cos\left(\frac{\pi}{4}-\phi_1\right)} \to 0 \qquad \Rightarrow \boxed{\phi_1 \in \left(-\frac{\pi}{4}, \frac{3\pi}{4}\right)}$$

$$u_{22} \to 0 \implies Y_{2,1}^{[-1]} \cong e^{-\sqrt{2}m_1 \cos\left(\frac{\pi}{4}+\phi_1\right)} \to 0 \qquad \Rightarrow \boxed{\phi_1 \in \left(-\frac{3\pi}{4}, \frac{\pi}{4}\right)}$$

Since the remaining cross ratios involve values of the Y-functions outside the fundamental strip we must use the recursion relations (3.10). This gives:

$$u_{21}\to 0 \quad\Longrightarrow\quad Y_{2,2}^{[-2]} = \frac{1+Y_{2,1}^{[-1]}}{Y_{2,2}^{[0]}\left(1+\frac{1}{Y_{3,2}^{[-1]}}\right)\left(1+\frac{1}{Y_{1,2}^{[-1]}}\right)}$$
$$\cong \frac{e^{\sqrt{2}m_2\cos\phi_2}}{\left(1+e^{m_2\cos\left(\frac{\pi}{4}+\phi_2\right)-C_2}\right)\left(1+e^{m_2\cos\left(\frac{\pi}{4}+\phi_2\right)+C_2}\right)}\to 0$$
$$\Rightarrow \boxed{\phi_2\in(-\pi,0)\cup\left(\frac{\pi}{2},\pi\right)}$$

$$u_{11}\to 1 \quad\Longrightarrow\quad Y_{2,2}^{[2]} = \frac{1+Y_{2,1}^{[1]}}{Y_{2,2}^{[0]}\left(1+\frac{1}{Y_{3,2}^{[1]}}\right)\left(1+\frac{1}{Y_{1,2}^{[1]}}\right)}$$
$$\cong \frac{e^{\sqrt{2}m_2\cos\phi_2}}{\left(1+e^{m_2\cos\left(\frac{\pi}{4}-\phi_2\right)-C_2}\right)\left(1+e^{m_2\cos\left(\frac{\pi}{4}-\phi_2\right)+C_2}\right)}\to\infty$$
$$\Rightarrow \boxed{\phi_2\in\left(-\frac{\pi}{2},0\right)}$$

To determine the precise values of ϕ_s in the multi-Regge limit, we look at the ratios (2.30)

$$\frac{u_{22}}{u_{32}}\to\text{const.} \quad\Longrightarrow\quad \frac{Y_{2,1}^{[-1]}}{Y_{2,1}^{[1]}} = \frac{e^{-\sqrt{2}m_1\cos\left(\frac{\pi}{4}+\phi_1\right)}}{e^{-\sqrt{2}m_1\cos\left(\frac{\pi}{4}-\phi_1\right)}} = e^{2m_1\sin\phi_1}\to\text{const.}\Rightarrow\boxed{\phi_1\to 0}$$

$$\frac{u_{21}}{u_{31}}\to\text{const.} \quad\Longrightarrow\quad \frac{Y_{2,2}^{[-2]}}{Y_{2,2}^{[0]}} = \frac{e^{2\sqrt{2}m_2\cos\phi_2}}{\left(1+e^{m_2\cos\left(\frac{\pi}{4}+\phi_2\right)-C_2}\right)\left(1+e^{m_2\cos\left(\frac{\pi}{4}+\phi_2\right)+C_2}\right)}\to\text{const.}$$
$$\Rightarrow \boxed{\phi_2\to-\frac{\pi}{4}}$$

B Residue structure for arbitrary Y-functions

As mentioned in the text, the residue structure for Y-functions with large shifts is intricate. In this section, we will demonstrate how the residue structure can be read off from the pattern introduced in the text. To do so, we will look at the specific example $Y_{2,1}^{[-4]}$. The phases that appear in the Y-system equation are $\phi_1=0$ and $\phi_2=-\pi/4$. Since we need to evaluate our Y-function at $\theta=-i\pi$, the quantity $\theta-i\phi_1$ crosses the poles $-i\frac{\pi}{4}, -i\frac{\pi}{2}, -i\frac{3}{4}\pi$, while $\theta-i\phi_2$ crosses $-i\frac{\pi}{4}, -i\frac{\pi}{2}$. The resulting residue structure therefore reads

$$Y_{2,1}^{[-4]} = \epsilon_1^{-\sqrt{2}}\cdot\underbrace{\frac{\left(1+Y_{2,2}^{[-3]}\right)}{\left(1+Y_{3,1}^{[-3]}\right)\left(1+Y_{1,1}^{[-3]}\right)}}_{\text{Residues at } -i\frac{\pi}{4}}\cdot\underbrace{\frac{\left(1+Y_{3,2}^{[-2]}\right)\left(1+Y_{1,2}^{[-2]}\right)}{\left(1+Y_{2,1}^{[-2]}\right)^2}}_{\text{Residues at } -i\frac{\pi}{2}}\cdot\underbrace{\frac{1}{\left(1+Y_{3,1}^{[-1]}\right)\left(1+Y_{1,1}^{[-1]}\right)}}_{\text{Residues at } -i\frac{3}{4}\pi}\cdot \tag{B.1}$$

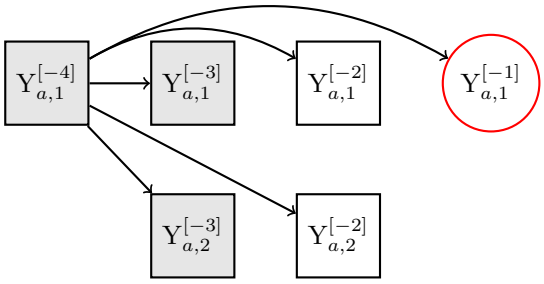

Figure 5. Residue structure of $Y_{a,1}^{[-4]}$. For simplicity, the residue dependencies of the other Y-functions are not shown.

Graphically, this residue structure can be represented as in figure 5, which remains valid for $Y_{a,1}^{[-4]}$. Of course, some of the Y-functions that appear as residues themselves receive corrections from residue terms, for example $Y_{2,2}^{[-3]}$ in the above example. However, it should be clear from the graphical representation that the residue term with the highest s' that can contribute to a Y-function $\mathrm{Y}_{a,s}^{[k]}$ with k negative is given by the intersection of the diagonal $\mathrm{Y}_{a,s+i}^{[k+i]}$ with the diagonal $\mathrm{Y}_{a,j}^{[-j]}$.

C 9-point multi-Regge limit

Here we present the equations governing the Y-system in the multi-Regge limit. In the lower half of the fundamental strip $\mathrm{Im}\theta \in (-\pi/4, 0)$ the equations are actually obtained simply by dropping the integral contributions from the original expressions (3.2)-(3.4). For the upper half of the fundamental strip $\mathrm{Im}\theta \in (0, \pi/4)$, some residue terms survive in the multi-Regge limit. The relevant equations take the form $\log \mathrm{Y}_{a,s} = p_{a,s}$ with the right hand side given by

$$p_{2\pm1,s}(\theta) = -m_s \cosh(\theta - i\phi_s) \pm C_s$$

$$p_{2,s}(\theta) = -\sqrt{2} m_s \cosh(\theta - i\phi_s)$$

for the first two values $s = 1, 2$ of the parameter s. Recall that the corresponding phases ϕ_s are given by $\phi_1 = 0$ and $\phi_2 = -\pi/4$. All the remaining functions contain residue terms. These are:

$$p_{2\pm1,3}(\theta) = -m_3 \cosh\left(\theta + i\frac{\pi}{2}\right) \pm C_3 + \log\left(1 + e^{\pm C_4 - m_4 \cosh\left(\theta + i\frac{\pi}{2}\right)}\right)$$

$$p_{2,3}(\theta) = -\sqrt{2} m_3 \cosh\left(\theta + i\frac{\pi}{2}\right) + \log\left(1 + e^{-\sqrt{2} m_4 \cosh\left(\theta + i\frac{\pi}{2}\right)}\right)$$

$$p_{2\pm1,4}(\theta) = -m_4 \cosh\left(\theta + i\frac{3\pi}{4}\right) \pm C_4 - \log\left(1 + e^{-\sqrt{2} m_4 \cosh\left(\theta + i\frac{\pi}{2}\right)}\right)$$

$$p_{2,4}(\theta) = -\sqrt{2} m_4 \cosh\left(\theta + i\frac{3\pi}{4}\right) - \log\left(\left(1 + e^{C_4 - m_4 \cosh\left(\theta + i\frac{\pi}{2}\right)}\right)\left(1 + e^{-C_4 - m_4 \cosh\left(\theta + i\frac{\pi}{2}\right)}\right)\right)$$

As mentioned in the text, these equations could be used as the starting point to find the solutions of equation (6.6) numerically. If we use the above functions $p_{a,s}$, however, the left-hand side of

eqs. (6.6) involve sums of products of exponentials such as

$$e^{p_{2,3}(\theta)} = e^{-\sqrt{2}m_3 \cosh\left(\theta + i\frac{\pi}{2}\right)} \left(1 + e^{-\sqrt{2}m_4 \cosh\left(\theta + i\frac{\pi}{2}\right)}\right) \ .$$

In order for the Bethe ansatz equations to take a more standard form one needs to work with a larger set of momenta p_A and the corresponding S matrices as discussed in the main text.

References

[1] J. M. Drummond, J. Henn, G. P. Korchemsky, and E. Sokatchev, *Conformal Ward identities for Wilson loops and a test of the duality with gluon amplitudes*, *Nucl. Phys.* **B826** (2010) 337–364, [arXiv:0712.1223].

[2] J. M. Maldacena, *The large N limit of superconformal field theories and supergravity*, *Adv. Theor. Math. Phys.* **2** (1998) 231–252, [hep-th/9711200].

[3] Z. Bern, L. J. Dixon, and V. A. Smirnov, *Iteration of planar amplitudes in maximally supersymmetric Yang-Mills theory at three loops and beyond*, *Phys. Rev.* **D72** (2005) 085001, [hep-th/0505205].

[4] L. F. Alday and J. M. Maldacena, *Gluon scattering amplitudes at strong coupling*, *JHEP* **06** (2007) 064, [arXiv:0705.0303].

[5] J. M. Drummond, J. Henn, G. P. Korchemsky, and E. Sokatchev, *The hexagon Wilson loop and the BDS ansatz for the six- gluon amplitude*, *Phys. Lett.* **B662** (2008) 456–460, [arXiv:0712.4138].

[6] Z. Bern *et. al.*, *The Two-Loop Six-Gluon MHV Amplitude in Maximally Supersymmetric Yang-Mills Theory*, *Phys. Rev.* **D78** (2008) 045007, [arXiv:0803.1465].

[7] J. Bartels, L. N. Lipatov, and A. Sabio Vera, *BFKL Pomeron, Reggeized gluons and Bern-Dixon-Smirnov amplitudes*, *Phys. Rev.* **D80** (2009) 045002, [arXiv:0802.2065].

[8] J. Bartels, L. N. Lipatov, and A. Sabio Vera, *$\mathcal{N} = 4$ supersymmetric Yang Mills scattering amplitudes at high energies: the Regge cut contribution*, *Eur. Phys. J.* **C65** (2010) 587–605, [arXiv:0807.0894].

[9] A. B. Goncharov, M. Spradlin, C. Vergu, and A. Volovich, *Classical Polylogarithms for Amplitudes and Wilson Loops*, [arXiv:1006.5703].

[10] V. Del Duca, C. Duhr, and V. A. Smirnov, *An Analytic Result for the Two-Loop Hexagon Wilson Loop in N = 4 SYM*, *JHEP* **03** (2010) 099, [arXiv:0911.5332].

[11] V. Del Duca, C. Duhr, and V. A. Smirnov, *The Two-Loop Hexagon Wilson Loop in N = 4 SYM*, *JHEP* **05** (2010) 084, [arXiv:1003.1702].

[12] L. N. Lipatov and A. Prygarin, *Mandelstam cuts and light-like Wilson loops in $\mathcal{N} = 4$ SUSY*, [arXiv:1008.1016].

[13] L. J. Dixon, J. M. Drummond and J. M. Henn, JHEP **1111** (2011) 023, [arXiv:1108.4461].

[14] S. Caron-Huot and S. He, *Jumpstarting the All-Loop S-Matrix of Planar N=4 Super Yang-Mills*, [arXiv:1112.1060].

[15] L. J. Dixon, C. Duhr and J. Pennington, *Single-valued harmonic polylogarithms and the multi-Regge limit*, [arXiv:1207.0186].

[16] L. J. Dixon, C. Duhr and J. Pennington, to appear.

[17] V. S. Fadin and L. N. Lipatov, Phys. Lett. B **706** (2012) 470, [arXiv:1111.0782].

[18] L. N. Lipatov and A. Prygarin, *BFKL approach and six-particle MHV amplitude in N=4 super Yang-Mills* Phys. Rev. D **83** (2011) 125001, [arXiv:1011.2673].

[19] J. Bartels, A. Kormilitzin, L. N. Lipatov and A. Prygarin, [arXiv:1112.6366].

[20] L. N. Lipatov, *Integrability of scattering amplitudes in $\mathcal{N} = 4$ SUSY*, *J. Phys.* **A42** (2009) 304020, [arXiv:0902.1444].

[21] L. F. Alday and J. Maldacena, *Null polygonal Wilson loops and minimal surfaces in Anti-de-Sitter space*, *JHEP* **11** (2009) 082, [arXiv:0904.0663].

[22] L. F. Alday, D. Gaiotto, and J. Maldacena, *Thermodynamic Bubble Ansatz*, [arXiv:0911.4708].

[23] L. F. Alday, J. Maldacena, A. Sever, and P. Vieira, *Y-system for Scattering Amplitudes*, arXiv:1002.2459.

[24] J. Bartels, J. Kotanski and V. Schomerus, *Excited Hexagon Wilson Loops for Strongly Coupled $\mathcal{N} = 4$ SYM*, *JHEP***1101** (2011) 096, [arXiv:1009.3938].

[25] P. Dorey and R. Tateo, *Excited states by analytic continuation of TBA equations*, *Nucl. Phys.* **B482** (1996) 639–659, [hep-th/9607167].

[26] P. Dorey and R. Tateo, *Excited states in some simple perturbed conformal field theories*, *Nucl. Phys.* **B515** (1998) 575–623, [hep-th/9706140].

[27] Y. Hatsuda, K. Ito, K. Sakai, and Y. Satoh, *Six-point gluon scattering amplitudes from Z_4-symmetric integrable model*, *JHEP* **09** (2010) 064, [arXiv:1005.4487].

[28] Y. Hatsuda, K. Ito, K. Sakai and Y. Satoh, *g-functions and gluon scattering amplitudes at strong coupling*, JHEP **1104** (2011) 100 [arXiv:1102.2477].

[29] Y. Hatsuda, K. Ito and Y. Satoh, *T-functions and multi-gluon scattering amplitudes*, JHEP **1202** (2012) 003 [arXiv:1109.5564].

[30] L. F. Alday, D. Gaiotto, J. Maldacena, A. Sever, and P. Vieira, *An Operator Product Expansion for Polygonal null Wilson Loops*, arXiv:1006.2788.

[31] D. Gaiotto, J. Maldacena, A. Sever and P. Vieira, *Bootstrapping Null Polygon Wilson Loops*, JHEP **1103** (2011) 092 [arXiv:1010.5009].

[32] D. Gaiotto, J. Maldacena, A. Sever and P. Vieira, JHEP **1112** (2011) 011 [arXiv:1102.0062].

[33] J. Bartels, L. N. Lipatov and A. Prygarin, *Collinear and Regge behavior of $2 \to 4$ MHV amplitude in $N = 4$ super Yang-Mills theory*, arXiv:1104.4709 [hep-th].

[34] R. C. Brower, C. E. DeTar and J. H. Weis, *Regge Theory for Multiparticle Amplitudes* Phys. Rept. **14** (1974) 257.

[35] G. Yang, *A simple collinear limit of scattering amplitudes at strong coupling*, *JHEP*, **1103** (2011) 87 [arXiv:1006.3306].

[36] D. Gaiotto, G. W. Moore and A. Neitzke, *Wall-crossing, Hitchin Systems, and the WKB Approximation*, [arXiv:0907.3987].

[37] D. Gaiotto, G. W. Moore and A. Neitzke, *Spectral networks*, [arXiv:1204.4824].

[38] J. Bartels, Nucl. Phys. B **175** (1980) 365,
J. Kwiecinski and M. Praszalowicz, Phys. Lett. B **94** (1980) 413.

[39] J. Bartels, L. N. Lipatov and A. Prygarin, *Integrable spin chains and scattering amplitudes*, J. Phys. A A **44** (2011) 454013, [arXiv:1104.0816].